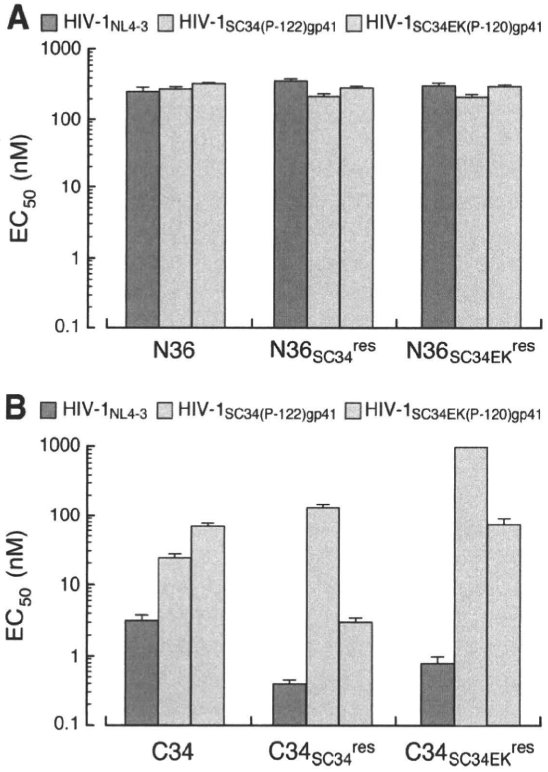

FIGURE 5. **Antiviral activity of resistant mutation-introduced peptides.** Antiviral activity of resistant mutation-introduced N36 ($N36_{SC34}^{res}$, $N36_{SC34EK}^{res}$, and original N36) (*A*) or C34 ($C34_{SC34}^{res}$, $C34_{SC34EK}^{res}$, and original C34) peptides (*B*) against HIV-1_{NL4-3} (*blue*), HIV-$1_{SC34(P-122)gp41}$ (*pink*), and HIV-$1_{SC34EK(P-120)gp41}$ (*green*) was determined using the MAGI assay. Peptide sequences are shown in Fig. 4*A*. HIV-1_{NL4-3} was used as the wild-type virus. HIV-$1_{SC34(P-122)gp41}$ contained D36G/I37K/R46K/Q52R/Q56R/N126K/S138A/E151K/K154N/N163D/L204I/L210F mutations. HIV-$1_{SC34EK(P-120)gp41}$ had D36G/Q41R/N43K/A96D/N126K/H132Y/V182I/P203S/L204I/S241F/H258Q/A312T mutations. Data are shown as mean EC_{50} values with *error bars* indicating standard deviations, obtained from at least three independent experiments.

ity and result in thermal instability of the 6-helix bundle by destabilizing the N-HR·C-HR complex. In contrast, mutations in C-HR simply enhanced the binding affinity to both wild-type and mutated N-HR.

Inhibitory Activity of Modified Fusion Inhibitors—We have previously demonstrated that introduction of resistance mutations to T-20 restores anti-HIV-1 activity against T-20-resistant variants (18), suggesting that this strategy can result in the design of peptides with improved potential for the treatment of resistant HIV-1. We examined whether this strategy was also applicable to SC34- and SC34EK-selected mutations. Hence, we introduced SC34- and SC34EK-resistant mutations that emerged in N-HR or C-HR, into the parental N36 or C34 peptides, respectively (Fig. 4*A*). Anti-HIV activities of both $N36_{SC34}^{res}$ and $N36_{SC34EK}^{res}$ showed little change compared with N36 (Fig. 5*A*), consistent with the CD analyses shown in Fig. 4, *B* and *C*, whereas mutations introduced into C34 restored their activity (Fig. 5*B*). $C34_{SC34}^{res}$ showed potent activity against HIV-1_{NL4-3} and surprisingly, it also exhibited enhanced activity against HIV-$1_{SC34EK(P-120)gp41}$. $C34_{SC34EK}^{res}$ moderately suppressed HIV-$1_{SC34EK(P-120)gp41}$, but was more effective in suppressing HIV-1_{NL4-3}, as compared with C34.

TABLE 3

Antiviral activity of fusion inhibitors to SC34- and SC34EK-selected mutation introduced HIV-1 gp41 recombinant viruses

Anti-HIV activity was determined using MAGI assay. Data are shown as mean ± S.D. obtained from at least three independent experiments, and resistance (*n*-fold of EC_{50}) of recombinant viruses, compared to that of parental HIV-1_{NL4-3}, is shown in parentheses.

Inhibitors	EC_{50} (nM)		
	HIV-1_{NL4-3} [a]	HIV-$1_{SC34(P-122)gp41}$ [b]	HIV-$1_{SC34EK(P-120)gp41}$ [c]
T-1249	0.4 ± 0.07	0.5 ± 0.06 (1.3)	0.5 ± 0.03 (1.3)
T-2410	1.0 ± 0.3	38 ± 13 (38)	3.7 ± 0.6 (3.7)
T-2429	2.2 ± 0.8	5.9 ± 1.3 (2.7)	5.4 ± 1.1 (2.5)
T-2544	0.9 ± 0.3	1.5 ± 0.5 (1.7)	1.4 ± 0.5 (1.6)
T-2635	0.3 ± 0.08	0.4 ± 0.1 (1.3)	1.1 ± 0.2 (3.7)
T-290676	0.7 ± 0.2	2.9 ± 0.8 (4.1)	4.6 ± 0.6 (6.6)
Sifuvirtide	1.7 ± 0.5	340 ± 55 (200)	35 ± 8.3 (21)
T-20EK	6.4 ± 0.8	1,548 ± 90 (242)	2,650 ± 261 (414)

[a] HIV-1_{NL4-3} was used as wild-type virus.
[b] HIV-$1_{SC34(P-122)gp41}$ has D36G/I37K/R46K/Q52R/Q56R/N126K/S138A/E151K/K154N/N163D/L204I/L210F mutations.
[c] HIV-$1_{SC34EK(P-120)gp41}$ has D36G/Q41R/N43K/A96D/N126K/H132Y/V182I/P203S/L204I/S241F/H258Q/A312T mutations.

These results further validate our strategy to overcome resistance to peptide fusion inhibitors by incorporating resistance mutations into the sequence of the original peptide inhibitor. Hence, we have been able to design peptides that can overcome resistance to T-20, C34, and now SC34 and SC34EK.

Inhibition of Resistant HIV-1 by Peptide Fusion Inhibitors—Recently, several novel peptides, including SC34 and SC34EK, have been developed as the next generation fusion inhibitors. To compare their antiviral properties, we evaluated their activities against SC34- and SC34EK-resistant HIV-1. All tested peptide fusion inhibitors showed remarkable anti-HIV-1 activity against HIV-1_{NL4-3} with EC_{50} values in the subnanomolar to nanomolar range (Table 3). However, the inhibitors had different effects on SC34- and SC34EK-resistant variants. T-1249, T-2429, T-2544, T-2635, and T-290676 retained activity against HIV-$1_{SC34(P-122)gp41}$, whereas T-2410, sifuvirtide, and T-20EK showed a decreased effect to various extents. Similarly, sifuvirtide and T-20EK had reduced activity against HIV-$1_{SC34EK(P-120)gp41}$. These results indicate that only minimal cross-resistance to the next generation of fusion inhibitors might emerge, and suggest possible successful combinations of fusion inhibitors.

DISCUSSION

To date, it remains unclear how the electrostatic constraints that are imposed on a peptide by the incorporation of EK motifs also affect the resistance profile and other virological features of these peptide fusion inhibitors. In this study, we selected HIV variants to the SC34 and SC34EK peptide inhibitors that have EK motifs, and compared their resistance profiles by comprehensive mutational analysis. SC34 and SC34EK selected several mutations within the gp41- and gp120-coding sequences over a period greater than 1 year. Phenotypic and replication kinetics analyses revealed that in the case of both inhibitors, changes in gp41 sequences served as primary mutations that decreased resistance to the inhibitors, whereas the changes in gp120 were secondary mutations compensatory in nature. However, the mutated regions of gp41 of the selected SC34- and SC34EK-resistant viruses were considerably different; mutations selected by SC34 were

mostly located within N-HR and C-HR, whereas more than half of those by SC34EK were located in another region of gp41. The molecular mechanisms and interactions that determine the effects of gp41 mutations outside the HRs on HIV-1 replication kinetics and the fusion process are not well understood. Therefore, further biological and structural studies focused on such interactions may reveal novel insights into the mechanism of fusion and the inhibition by drugs that target HIV-1 fusion.

SC34EK was designed to possess unidirectionally aligned EK pairs by modifying SC34 to have the two reverse-oriented EK pairs (Fig. 1). Thus, the difference in peptide sequences induced a different resistance pattern and reduced cross-resistance. Although accumulation of multiple mutations in gp41 eventually conferred a high level of resistance to SC34 and SC34EK, susceptibility to both inhibitors was not significantly affected by single amino acid substitutions. Moreover, it has been reported that substitutions in gp120 modulate the susceptibility to T-20 (33–36), and we also observed that both SC34- and SC34EK-selected mutations in the gp120 conferred resistance to T-20 but not to SC34 and SC34EK. These results indicate that SC34 and SC34EK have a high genetic barrier of resistance.

One mutation appeared to contribute significantly to the reduced cross-resistance of SC34- and SC34EK-resistant variants. Specifically, SC34EK selected the N43K mutation, whereas T-20 selected for N43D (31, 37), which is frequently observed together with E137K, a compensatory mutation in C-HR that maintains interaction with the N43D-substituted N-HR, possibly through the Asp^{43}-Lys^{137} ion pair (38, 39). SC34EK has been designed to harbor Lys^{137} in its peptide sequence. Hence, it is possible that resistance to SC34EK emerges through unfavorable repulsive charge-charge interactions between the Lys^{43} of the viral N-HR and the Lys^{137} residue of SC34EK. Therefore, charge interactions between amino acids 43 and 137 are likely to be the mechanism for resistance to T-20 and in part to SC34EK, but not to SC34, which has a glutamic acid (Glu^{43}) at this position. This might be one of the reasons why SC34 and SC34EK did not show significant cross-resistance.

We recently demonstrated that $T\text{-}20_{S138A}$ and $C34_{N126K}$ are able to suppress T-20- and C34-resistant variants, respectively (18). We again applied the same strategy and introduced resistance mutations in SC34 and SC34EK and examined the effect of these changes on their potency against SC34- or SC34EK-resistant variants. In this case, only mutations in the C-HR conferred enhanced susceptibility by augmenting binding affinity to the target N-HR. In the case of the $C34_{SC34EK}{}^{res}$ peptide, although we expected minimal impact of H132Y on drug susceptibility and/or on C-HR conformation, S138A appeared to stabilize the 6-helix complex by improving hydrophobic contacts with the pocket formed by Leu^{44} and Leu^{45}, as reported previously (18). In the case of the $C34_{SC34}{}^{res}$ peptide, in addition to the aforementioned S138A effect, it was expected that N126K would enable the formation of possible intra-helical salt bridges with Glu^{123} that would stabilize the α-helicity of C-HR. These mutations improved the anti-HIV-1 activity toward wild-type, and surprisingly, to SC34EK-resistant variants as well.

A number of potent peptide fusion inhibitors that suppress T-20-resistant variants have been previously reported (13, 14, 40, 41). Resistance profiles of these next generation fusion inhibitors with physicochemical modifications are expected to be different from those of the native sequence peptide fusion inhibitors, although only those of T-1249 and T-2635 were examined (42, 43). T-1249, one of the first next generation fusion inhibitors, showed potent anti-HIV-1 activity in HIV-1-infected patients that failed to respond to T-20 treatment (12). However, mutations at positions 36–45 (such as V38A/E, Q40H/K, and N43D/K), which are also observed in T-20-resistant variants *in vitro* and *in vivo*, were also detected in clinical trials of T-1249 (12, 44, 45). Nearly all the individual selected mutations had little impact on the susceptibility to T-1249. However, V38D/E conferred high-level resistance to T-1249 (30-fold) and T-20 (more than 200-fold), but not to another fusion inhibitor, T-2635 (42, 43), suggesting that there is potential cross-resistance between T-20 and T-1249. In contrast, T-2635 was hardly affected by such single mutations except for Q79E and K90E with a mild resistance of 4- and 7-fold, respectively (42), indicating that T-2635 had a preferential resistance pattern similar to SC34 and SC34EK, because these inhibitors were essentially effective against all variants with single mutations. Interestingly, although HIV-$1_{SC34(P\text{-}122)}$ and HIV-$1_{SC34EK(P\text{-}120)}$ showed mild (7.3-fold) and moderate resistance (21-fold) to C34, respectively, we observed significant differences in resistance against T-2410, another next generation fusion inhibitor, which differed from C34 by only two added amino acids at each of the N and C termini (13). Specifically, the susceptibilities of HIV-$1_{SC34(P\text{-}122)gp41}$ and HIV-$1_{SC34EK(P\text{-}120)gp41}$ to T-2410 were decreased by 38- and 3.7-fold, respectively. Although the mechanism underlying the ineffectiveness of T-2410 against SC34-resistant HIV-1 remains unclear, it appears that the size of the peptide inhibitor may be another parameter that should be considered in future attempts to design fusion peptide inhibitors with improved resistance profiles. Meanwhile, sifuvirtide and T-20EK did not show anti-HIV-1 activity against either SC34- or SC34EK-resistant variants, suggesting that they may partially share a common resistance profile. Sifuvirtide was designed based on the sequence of the C34 region of gp41 derived from HIV-1 subtype E. Similar to SC34 and SC34EK, sifuvirtide includes amino acid substitutions that could form intramolecular salt bridges. However, the majority of amino acids in sifuvirtide must be bound to the same region of N-HR, where C34, SC34, and SC34EK may interact (14). This may explain why sifuvirtide was inactive against SC34- and SC34EK-resistant variants. T-20 derivatives, including T-20EK, lack the N-terminal tryptophan-rich domain (N-TRD), also known as the pocket-binding domain, that interacts with the hydrophobic groove of the N-HR trimer (46), but they have the C-terminal TRD that interacts with the lipid bilayer at the cellular membrane (47). Our results showed that T-20-derived peptides seem less active compared with C34 derivatives with N-TRD. Recently, treatment with two or three fusion inhibitors was reported to have a potent and syn-

ergistic antiviral activity on T-20-resistant variants (48, 49). Together, these observations indicated that each inhibitor has a distinct inhibitory mechanism that may lead to the design of a combination therapy of fusion inhibitors *in vivo*.

In conclusion, the barrier for resistance to SC34 and SC34EK is considerably higher than that for the parent compound C34, or for T-20. Moreover, these inhibitors have a distinct resistance profile from C34, T-20, and other next generation fusion inhibitors. Hence, they are excellent alternatives for clinical use. Although mutations induced by SC34 and SC34EK are partially overlapped, most mutations were specific to each agent. Importantly, we demonstrated that interchange of only two pairs of EK positions could reduce cross-resistance. Because sites and direction of the EK modification seem to be easily replaceable, this is a useful strategy to suppress more efficiently emergence of resistant variants. Moreover, the present study demonstrates that the usefulness of this strategy that we have previously applied to design improved fusion inhibitors with HIV-1 sequences (18) has been extended to improve fusion inhibitors with "artificial" (non-HIV) sequences.

REFERENCES

1. Gallo, S. A., Finnegan, C. M., Viard, M., Raviv, Y., Dimitrov, A., Rawat, S. S., Puri, A., Durell, S., and Blumenthal, R. (2003) *Biochim. Biophys. Acta* **1614,** 36–50
2. Berger, E. A., Murphy, P. M., and Farber, J. M. (1999) *Annu. Rev. Immunol.* **17,** 657–700
3. Epand, R. M. (2003) *Biochim. Biophys. Acta* **1614,** 116–121
4. Chan, D. C., Fass, D., Berger, J. M., and Kim, P. S. (1997) *Cell* **89,** 263–273
5. Ryser, H. J., and Flückiger, R. (2005) *Drug Discov. Today* **10,** 1085–1094
6. O'Shea, E. K., Rutkowski, R., and Kim, P. S. (1989) *Science* **243,** 538–542
7. Wild, C., Oas, T., McDanal, C., Bolognesi, D., and Matthews, T. (1992) *Proc. Natl. Acad. Sci. U.S.A.* **89,** 10537–10541
8. Lalezari, J. P., Henry, K., O'Hearn, M., Montaner, J. S., Piliero, P. J., Trottier, B., Walmsley, S., Cohen, C., Kuritzkes, D. R., Eron, J. J., Jr., Chung, J., DeMasi, R., Donatacci, L., Drobnes, C., Delehanty, J., and Salgo, M. (2003) *N. Engl. J. Med.* **348,** 2175–2185
9. Lazzarin, A., Clotet, B., Cooper, D., Reynes, J., Arasteh, K., Nelson, M., Katlama, C., Stellbrink, H. J., Delfraissy, J. F., Lange, J., Huson, L., DeMasi, R., Wat, C., Delehanty, J., Drobnes, C., and Salgo, M. (2003) *N. Engl. J. Med.* **348,** 2186–2195
10. Mink, M., Mosier, S. M., Janumpalli, S., Davison, D., Jin, L., Melby, T., Sista, P., Erickson, J., Lambert, D., Stanfield-Oakley, S. A., Salgo, M., Cammack, N., Matthews, T., and Greenberg, M. L. (2005) *J. Virol.* **79,** 12447–12454
11. Xu, L., Pozniak, A., Wildfire, A., Stanfield-Oakley, S. A., Mosier, S. M., Ratcliffe, D., Workman, J., Joall, A., Myers, R., Smit, E., Cane, P. A., Greenberg, M. L., and Pillay, D. (2005) *Antimicrob. Agents Chemother.* **49,** 1113–1119
12. Lalezari, J. P., Bellos, N. C., Sathasivam, K., Richmond, G. J., Cohen, C. J., Myers, R. A., Jr., Henry, D. H., Raskino, C., Melby, T., Murchison, H., Zhang, Y., Spence, R., Greenberg, M. L., Demasi, R. A., and Miralles, G. D. (2005) *J. Infect. Dis.* **191,** 1155–1163
13. Dwyer, J. J., Wilson, K. L., Davison, D. K., Freel, S. A., Seedorff, J. E., Wring, S. A., Tvermoes, N. A., Matthews, T. J., Greenberg, M. L., and Delmedico, M. K. (2007) *Proc. Natl. Acad. Sci. U.S.A.* **104,** 12772–12777
14. He, Y., Xiao, Y., Song, H., Liang, Q., Ju, D., Chen, X., Lu, H., Jing, W., Jiang, S., and Zhang, L. (2008) *J. Biol. Chem.* **283,** 11126–11134
15. Nishikawa, H., Nakamura, S., Kodama, E., Ito, S., Kajiwara, K., Izumi, K., Sakagami, Y., Oishi, S., Ohkubo, T., Kobayashi, Y., Otaka, A., Fujii, N., and Matsuoka, M. (2009) *Int. J. Biochem. Cell Biol.* **41,** 891–899
16. Marqusee, S., and Baldwin, R. L. (1987) *Proc. Natl. Acad. Sci. U.S.A.* **84,** 8898–8902
17. Otaka, A., Nakamura, M., Nameki, D., Kodama, E., Uchiyama, S., Nakamura, S., Nakano, H., Tamamura, H., Kobayashi, Y., Matsuoka, M., and Fujii, N. (2002) *Angew. Chem. Int. Ed. Engl.* **41,** 2937–2940
18. Izumi, K., Kodama, E., Shimura, K., Sakagami, Y., Watanabe, K., Ito, S., Watabe, T., Terakawa, Y., Nishikawa, H., Sarafianos, S. G., Kitaura, K., Oishi, S., Fujii, N., and Matsuoka, M. (2009) *J. Biol. Chem.* **284,** 4914–4920
19. Watabe, T., Terakawa, Y., Watanabe, K., Ohno, H., Nakano, H., Nakatsu, T., Kato, H., Izumi, K., Kodama, E., Matsuoka, M., Kitaura, K., Oishi, S., and Fujii, N. (2009) *J. Mol. Biol.* **392,** 657–665
20. Aquaro, S., D'Arrigo, R., Svicher, V., Perri, G. D., Caputo, S. L., Visco-Comandini, U., Santoro, M., Bertoli, A., Mazzotta, F., Bonora, S., Tozzi, V., Bellagamba, R., Zaccarelli, M., Narciso, P., Antinori, A., and Perno, C. F. (2006) *J. Antimicrob. Chemother.* **58,** 714–722
21. Chibo, D., Roth, N., Roulet, V., Skrabal, K., Gooey, M., Carolan, L., Nicholls, J., Papadakis, A., and Birch, C. (2007) *AIDS* **21,** 1974–1977
22. Chackerian, B., Long, E. M., Luciw, P. A., and Overbaugh, J. (1997) *J. Virol.* **71,** 3932–3939
23. Adachi, A., Gendelman, H. E., Koenig, S., Folks, T., Willey, R., Rabson, A., and Martin, M. A. (1986) *J. Virol.* **59,** 284–291
24. Nameki, D., Kodama, E., Ikeuchi, M., Mabuchi, N., Otaka, A., Tamamura, H., Ohno, M., Fujii, N., and Matsuoka, M. (2005) *J. Virol.* **79,** 764–770
25. Naito, T., Izumi, K., Kodama, E., Sakagami, Y., Kajiwara, K., Nishikawa, H., Watanabe, K., Sarafianos, S. G., Oishi, S., Fujii, N., and Matsuoka, M. (2009) *Antimicrob. Agents Chemother.* **53,** 1013–1018
26. Shimura, K., Kodama, E., Sakagami, Y., Matsuzaki, Y., Watanabe, W., Yamataka, K., Watanabe, Y., Ohata, Y., Doi, S., Sato, M., Kano, M., Ikeda, S., and Matsuoka, M. (2008) *J. Virol.* **82,** 764–774
27. Oishi, S., Ito, S., Nishikawa, H., Watanabe, K., Tanaka, M., Ohno, H., Izumi, K., Sakagami, Y., Kodama, E., Matsuoka, M., and Fujii, N. (2008) *J. Med. Chem.* **51,** 388–391
28. Kuiken, C., Leitner, T., Foley, B., Hahn, B., Marx, P., McCutchan, F., Wolinsky, S., and Korber, B. (eds) (2008) *HIV Sequence Compendium,* Los Alamos National Laboratory, Theoretical Biology and Biophysics, Los Alamos, NM
29. Rimsky, L. T., Shugars, D. C., and Matthews, T. J. (1998) *J. Virol.* **72,** 986–993
30. Lu, J., Deeks, S. G., Hoh, R., Beatty, G., Kuritzkes, B. A., Martin, J. N., and Kuritzkes, D. R. (2006) *J. Acquir. Immune Defic. Syndr.* **43,** 60–64
31. Melby, T., Sista, P., DeMasi, R., Kirkland, T., Roberts, N., Salgo, M., Heilek-Snyder, G., Cammack, N., Matthews, T. J., and Greenberg, M. L. (2006) *AIDS Res. Hum. Retroviruses* **22,** 375–385
32. Cabrera, C., Marfil, S., García, E., Martinez-Picado, J., Bonjoch, A., Bofill, M., Moreno, S., Ribera, E., Domingo, P., Clotet, B., and Ruiz, L. (2006) *AIDS* **20,** 2075–2080
33. Derdeyn, C. A., Decker, J. M., Sfakianos, J. N., Wu, X., O'Brien, W. A., Ratner, L., Kappes, J. C., Shaw, G. M., and Hunter, E. (2000) *J. Virol.* **74,** 8358–8367
34. Derdeyn, C. A., Decker, J. M., Sfakianos, J. N., Zhang, Z., O'Brien, W. A., Ratner, L., Shaw, G. M., and Hunter, E. (2001) *J. Virol.* **75,** 8605–8614
35. Reeves, J. D., Gallo, S. A., Ahmad, N., Miamidian, J. L., Harvey, P. E., Sharron, M., Pohlmann, S., Sfakianos, J. N., Derdeyn, C. A., Blumenthal, R., Hunter, E., and Doms, R. W. (2002) *Proc. Natl. Acad. Sci. U.S.A.* **99,** 16249–16254
36. Reeves, J. D., Miamidian, J. L., Biscone, M. J., Lee, F. H., Ahmad, N., Pierson, T. C., and Doms, R. W. (2004) *J. Virol.* **78,** 5476–5485
37. Sista, P. R., Melby, T., Davison, D., Jin, L., Mosier, S., Mink, M., Nelson, E. L., DeMasi, R., Cammack, N., Salgo, M. P., Matthews, T. J., and Greenberg, M. L. (2004) *AIDS* **18,** 1787–1794
38. Tolstrup, M., Selzer-Plön, J., Laursen, A. L., Bertelsen, L., Gerstoft, J., Duch, M., Pedersen, F. S., and Ostergaard, L. (2007) *AIDS* **21,** 519–521
39. Bai, X., Wilson, K. L., Seedorff, J. E., Ahrens, D., Green, J., Davison, D. K., Jin, L., Stanfield-Oakley, S. A., Mosier, S. M., Melby, T. E., Cammack, N., Wang, Z., Greenberg, M. L., and Dwyer, J. J. (2008) *Biochemistry* **47,** 6662–6670

40. He, Y., Cheng, J., Lu, H., Li, J., Hu, J., Qi, Z., Liu, Z., Jiang, S., and Dai, Q. (2008) *Proc. Natl. Acad. Sci. U.S.A.* **105,** 16332–16337
41. Qi, Z., Shi, W., Xue, N., Pan, C., Jing, W., Liu, K., and Jiang, S. (2008) *J. Biol. Chem.* **283,** 30376–30384
42. Eggink, D., Baldwin, C. E., Deng, Y., Langedijk, J. P., Lu, M., Sanders, R. W., and Berkhout, B. (2008) *J. Virol.* **82,** 6678–6688
43. Eggink, D., Langedijk, J. P., Bonvin, A. M., Deng, Y., Lu, M., Berkhout, B., and Sanders, R. W. (2009) *J. Biol. Chem.* **284,** 26941–26950
44. Melby, T., Demasi, R., Cammack, N., Miralles, G. D., and Greenberg, M. L. (2007) *AIDS Res. Hum. Retroviruses* **23,** 1366–1373
45. Eron, J. J., Gulick, R. M., Bartlett, J. A., Merigan, T., Arduino, R., Kilby, J. M., Yangco, B., Diers, A., Drobnes, C., DeMasi, R., Greenberg, M., Melby, T., Raskino, C., Rusnak, P., Zhang, Y., Spence, R., and Miralles, G. D. (2004) *J. Infect. Dis.* **189,** 1075–1083
46. Chan, D. C., Chutkowski, C. T., and Kim, P. S. (1998) *Proc. Natl. Acad. Sci. U.S.A.* **95,** 15613–15617
47. Salzwedel, K., West, J. T., and Hunter, E. (1999) *J. Virol.* **73,** 2469–2480
48. Pan, C., Cai, L., Lu, H., Qi, Z., and Jiang, S. (2009) *J. Virol.* **83,** 7862–7872
49. Pan, C., Lu, H., Qi, Z., and Jiang, S. (2009) *AIDS* **23,** 639–641

Bioorganic & Medicinal Chemistry Letters 20 (2010) 5853–5858

Contents lists available at ScienceDirect

Bioorganic & Medicinal Chemistry Letters

journal homepage: www.elsevier.com/locate/bmcl

CD4 mimics targeting the HIV entry mechanism and their hybrid molecules with a CXCR4 antagonist

Tetsuo Narumi [a], Chihiro Ochiai [a], Kazuhisa Yoshimura [b], Shigeyoshi Harada [b], Tomohiro Tanaka [a], Wataru Nomura [a], Hiroshi Arai [a], Taro Ozaki [a], Nami Ohashi [a], Shuzo Matsushita [b], Hirokazu Tamamura [a,*]

[a] Institute of Biomaterials and Bioengineering, Tokyo Medical and Dental University, Chiyoda-ku, Tokyo 101-0062, Japan
[b] Center for AIDS Research, Kumamoto University, Kumamoto 860-0811, Japan

ARTICLE INFO

Article history:
Received 14 June 2010
Revised 22 July 2010
Accepted 26 July 2010
Available online 3 August 2010

Keywords:
CD4
HIV entry
Hybrid molecule
gp120

ABSTRACT

Small molecules behaving as CD4 mimics were previously reported as HIV-1 entry inhibitors that block the gp120–CD4 interaction and induce a conformational change in gp120, exposing its co-receptor-binding site. A structure–activity relationship (SAR) study of a series of CD4 mimic analogs was conducted to investigate the contribution from the piperidine moiety of CD4 mimic **1** to anti-HIV activity, cytotoxicity, and CD4 mimicry effects on conformational changes of gp120. In addition, several hybrid molecules based on conjugation of a CD4 mimic analog with a selective CXCR4 antagonist were also synthesized and their utility evaluated.

The infection of host cells by HIV-1 takes place in multiple steps via a dynamic supramolecular mechanism mediated by two viral envelope glycoproteins (gp41, gp120) and several cell surface proteins (CD4, CCR5/CXCR4).[1] Cell penetration begins with the interaction of gp120 with the primary receptor CD4. This induces conformational changes in gp120, leading to the exposure of its V3 loop allowing the subsequent binding of gp120 to a co-receptor, CCR5[2] or CXCR4.[3]

N-(4-Chlorophenyl)-*N*′-(2,2,6,6-tetramethyl-piperidin-4-yl)oxalamide (NBD-556: **1**) and the related compounds NBD-557 (**2**) and YYA-021 (**3**) have been identified as a novel class of HIV-1 entry inhibitors, which exert potent cell fusion and virus cell fusion inhibitory activity at low micromolar levels (Fig. 1).[4] Furthermore, compound **1** can also induce thermodynamically favored conformational changes in gp120 similar to those caused by CD4 binding. The X-ray crystal structure of gp120 complexed with CD4 revealed the presence of a hydrophobic cavity, the Phe43 cavity, which is penetrated by the aromatic ring of Phe^{43} of CD4.[5] Molecular modeling revealed that compound **1** is also inserted into the Phe43 cavity, the *para*-chlorophenyl group of **1** entering more deeply than the phenyl ring of Phe^{43} of CD4 and interacting with the conserved gp120 residues such as Trp^{427}, Phe^{382}, and Trp^{112}.[4c] The modeling also suggested that an oxalamide linker forms hydrogen bonds with carbonyl groups of the gp120 backbone peptide bonds. Our model of **1** docked into gp120 revealed that eight other gp120 residues, Val^{255}, Asp^{368}, Glu^{370}, Ser^{375}, Ile^{424}, Trp^{427}, Val^{430}, and Val^{475} are located within a 4.4 Å-radius of **1** and that a large cavity exists around the *p*-position of the aromatic ring of **1**.[4e] Based on these observations, we conducted a structure–activity relationship (SAR) study of a series of analogs of CD4 mimics with substituents at the *p*-position of the aromatic ring. This study revealed that a certain size and electron-withdrawing ability of the substituents are indispensable for potent anti-HIV activity.[4e]

Although several reported SAR studies of **1** have revealed the contributions of the phenyl ring and the oxalamide linker of **1** to the binding affinity with gp120, the anti-HIV activity and the CD4 mimicry on conformational changes of gp120,[4] there has been, to the best of our knowledge, no prior report describing SAR studies of the piperidine ring of **1**. In this paper, the contributions of the piperidine ring of **1** to the anti-HIV activity, CD4 mimicry and cytotoxicity were investigated through the SAR studies focused on the piperidine ring of **1**. Furthermore, to apply the utility of CD4 mimics to the development of potent anti-HIV agents, a series of the

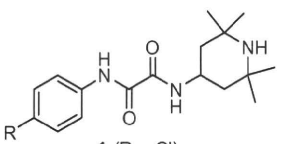

1 (R = Cl)
2 (R = Br)
3 (R = Me)

Figure 1. NBD-556 (**1**) and related compounds.

* Corresponding author.
E-mail address: tamamura.mr@tmd.ac.jp (H. Tamamura).

0960-894X/$ - see front matter © 2010 Elsevier Ltd. All rights reserved.
doi:10.1016/j.bmcl.2010.07.106

hybrid molecules that combined CD4 mimic analogs with a selective CXCR4 antagonist were also synthesized and bioevaluated.

For the design of novel CD4 mimic analogs, we initially tried to directly derivatize the nitrogen atom of piperidine group. However, direct alkylation and acylation of **1** failed probably as a result of steric hindrance from the methyl groups on the piperidine ring so we synthesized several derivatives lacking the methyl groups and evaluated their anti-HIV activity, cytotoxicity, and ability to mimic CD4. According to the previous SAR study,[4e] the *p*-Cl (**4**), *p*-Br (**5**) and *p*-methyl derivatives (**6**) lacking the methyl groups on the piperidine ring were prepared. Compounds **4–6** were synthesized by published methods as shown in Scheme 1. Briefly, coupling of aniline derivatives with ethyl chloroglyoxalate in the presence of Et_3N and subsequent saponification gave the corresponding acids (**10–12**). Condensation of these acids with 4-amino-*N*-benzylpiperidine in the presence of EDC–HOBt system, followed by debenzylation under von Braun conditions with 1-chloroethyl choroformate[6] produced the desired compounds **4–6**.[7]

The anti-HIV activity of each of the synthetic compounds was evaluated against MNA (R5) strain, with the results shown in Table 1. IC_{50} values were determined by the 3-(4,5-dimethylthiazol-2-yl)-2,5-diphenyltetrazolium bromide (MTT) method[8] as the concentrations of the compounds which conferred 50% protection against HIV-1-induced cytopathogenicity in PM1/CCR5 cells. Cytotoxicity of the compounds based on the viability of mock-infected PM1/CCR5 cells was also evaluated using the MTT method. CC_{50} values, the concentrations achieving 50% reduction of the viability of mock-infected cells, were also determined. Compounds **1** and **3** showed potent anti-HIV activity. The anti-HIV IC_{50} of compound **2** was previously reported to be comparable to that of compound **1**, and thus was not determined in this study. Novel derivatives **4** and **6** without the methyl groups on the piperidine ring, showed significant anti-HIV activity comparable to that of the parent compounds **1** and **3**, respectively. The *p*-methyl derivative **6** has slightly lower activity than the *p*-Cl derivative **4** and the *p*-Br derivative **5**. These results are consistent with our previous SAR studies on the parent compounds **1–3**. Compound **5** was found to exhibit relatively strong cytotoxicity (CC_{50} = 50 μM) and compounds **4** and **6** have cytotoxicities comparable to that of compounds **1** and **3**, respectively. This observation indicates that the methyl groups on the piperidine ring do not contribute significantly to the anti-HIV activity or the cytotoxicity.

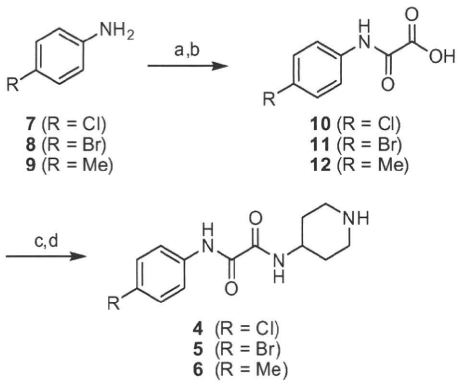

Scheme 1. Synthesis of compounds **4–6**. Reagents and conditions: (a) ethyl chloroglyoxylate, Et_3N, THF; (b) 1 M aq NaOH, THF, 67%–quant.; (c) 1-benzyl-4-aminopiperidine, EDC·HCl, $HOBt·H_2O$, Et_3N, THF; (d) (i) 1-chloroethyl chloroformate, CH_2Cl_2; (ii) MeOH, 8–47%.

Table 1
Effects of the methyl groups on anti-HIV activity and cytotoxicity of CD4 mimic analogs[a]

Compd	R	IC_{50} (μM) MNA (R5)	CC_{50} (μM)
1	Cl	12	110
2	Br	ND	93
3	Me	15	210
4	Cl	8	100
5	Br	6	50
6	Me	20	190

[a] All data with standard deviation are the mean values for at least three independent experiments (ND = not determined).

Compound **1** and the newly synthesized derivatives **4–6** were also evaluated for their effects on conformational changes of gp120 by a fluorescence activated cell sorting (FACS) analysis. The profile of binding of an anti-envelope CD4-induced monoclonal antibody (4C11) to the Env-expressing cell surface (an R5-HIV-1 strain, JR-FL, -infected PM1 cells) pretreated with the above derivatives was examined. Comparison of the binding of 4C11 to the cell surface was measured in terms of the mean fluorescence intensity (MFI), as shown in Figure 2. Pretreatment of the Env-expressing cell surface with compound **1** (MFI = 53.66) produced a significant increase in binding affinity for 4C11, consistent with that reported previously.[4e] This indicates that compound **1** enhances the binding affinity of gp120 with the 17b monoclonal antibody which recognizes CD4-induced epitopes on gp120. The Env-expressing cells without CD4 mimic-pretreatment failed to show significant binding affinity to 4C11. On the other hand, the profiles of the binding of 4C11 to the Env-expressing cell surface pretreated with compound **4** (Cl derivative) and **5** (Br derivative) (MFI = 49.88 and 52.34) were similar to that of compound **1**. Pretreatment of the cell surface with compound **6** (Me derivative) (MFI = 45.99) produced slightly lower enhancement but significant levels of binding affinity for 4C11, compared to that of compound **1** as pretreatments. These results suggested that the removal of the methyl groups on the piperidine moiety might not affect the CD4 mimicry effects on conformational changes of gp120 and it was conjectured that the phenyl ring of CD4 mimic might be a key moiety for the interaction with gp120 to induce the conformational changes of gp120. This is consistent with the results in the previous paper where it was reported that CD4 mimics having suitable substituent(s) on the phenyl ring cause a conformational change, resulting in external exposure of the co-receptor-binding site of gp120.[4e]

Based on these results, a series of N-alkylated and N-acylated piperidine derivatives **13–18** with no methyl groups were prepared. Several compounds with 6-membered rings were also prepared to determine whether or not the piperidine ring is mandatory. The synthesis of these derivatives is shown in Scheme 2. Since the *p*-Cl derivative **4** showed potent anti-HIV activity and relatively low cytotoxicity, compared to the *p*-Br derivative **5**, chlorine was selected as the substituent at the *p*-position of the phenyl ring. The N-methyl derivative **13** was synthesized by coupling of **10** with 4-amine-1-methylpiperidine. Alkylation of **4** with *tert*-butyl bromoacetate, followed by deprotection of *tert*-butyl ester provided compound **14**. The N-isopropyl derivative **15** was prepared by reductive amination of **4** with isopropyl aldehyde. The N-acyl derivatives **16–18** were prepared by simple acylation or condensation with the corresponding substrate. The synthesis of other derivatives **19–23** with different 6-membered rings is depicted in Scheme 3. The 6-membered ring derivatives with the exception of **21** were prepared by coupling of acid **10** with the corresponding amines. Compound **21** was prepared by reaction of **10** with thionyl chloride to give the corresponding acid chloride, which was subsequently coupled with 4-aminopyridine.

Compounds **1**, **3**, and **13–18** were evaluated for their CD4 mimicry effects on conformational changes of gp120 by the FACS anal-

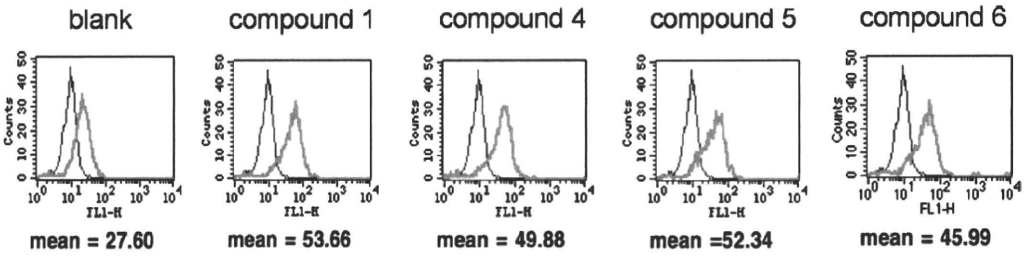

Figure 2. FACS analysis of compounds **1** and **4–6**. JR-FL (R5, Sub B) chronically infected PM1 cells were preincubated with 100 μM of a CD4 mimic for 15 min, and then incubated with an anti-HIV-1 mAb, 4C11, at 4 °C for 15 min. The cells were washed with PBS, and fluorescein isothiocyanate (FITC)-conjugated goat anti-human IgG antibody was used for antibody-staining. Flow cytometry data for the binding of 4C11 (green lines) to the Env-expressing cell surface in the presence of a CD4 mimic are shown among gated PM1 cells along with a control antibody (anti-human CD19:black lines). Data are representative of the results from a minimum of two independent experiments. The number at the bottom of each graph shows the mean fluorescence intensity (MFI) of the antibody 4C11.

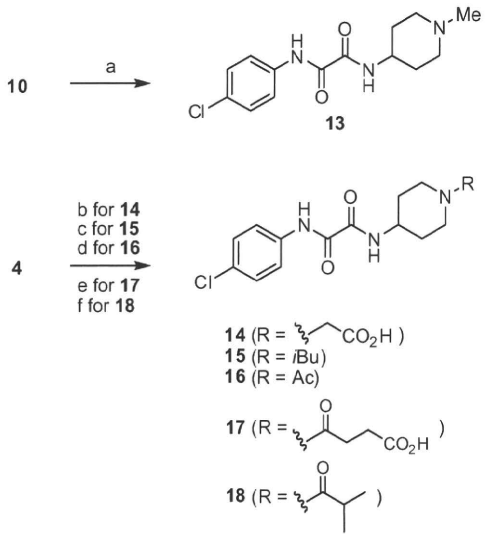

Scheme 2. Synthesis of N-alkylated and N-acylated piperidine derivatives **13–18**. Reagents and conditions: (a) 4-amine-1-methylpiperidine, EDC·HCl, HOBt·H_2O, Et_3N, THF, 16%; (b) (i) *tert*-butyl bromoacetate, NaH, DMF; (ii) TFA, 6%; (c) isobutylaldehyde, $NaBH(OAc)_3$, AcOH, DCE, quant.; (d) acetyl chloride, Et_3N, DMF, quant.; (e) succinic anhydride, Et_3N, THF, 37%; (f) isobutyric acid, EDC·HCl, HOBt·H_2O, Et_3N, THF, 95%.

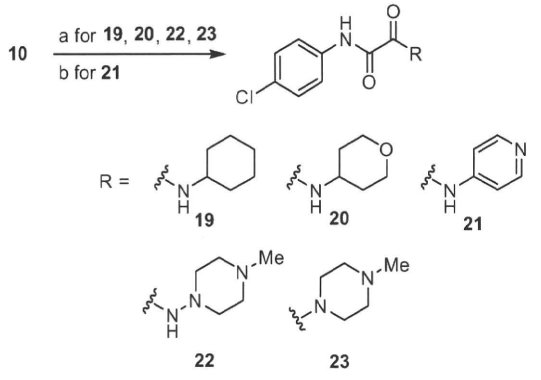

Scheme 3. Synthesis of 6-membered ring derivatives **19–23**. Reagents and conditions: (a) the corresponding amine, EDC·HCl, HOBt·H_2O, Et_3N, THF, 22%–quant.; (b) 4-aminopyridine, $SOCl_2$, MeOH, 38%.

ysis, and the results are shown in Figure 3. Pretreatment of the Env-expressing cells with the N-substituted compounds **13**, **15**, **16**, and **18** produced a notable increase in binding affinity to 4C11, similar to that observed in the pretreatment with compound **1**. The profile of the binding of 4C11 to the cell surface pretreated with compounds **14** and **17** was similar to that of controls, suggesting that these derivatives offer no significant enhancement of binding affinity for 4C11 and that the carboxylic moiety in the terminal of piperidine ring is not suited to CD4 mimicry. It is hypothesized that the carboxylic moieties of compounds **14** and **17** might prevent the interaction of CD4 mimic with gp120 by their multiple contacts with side chain(s) of amino acid(s) around the Phe43 cavity, such as Asp^{368} and Glu^{370}. Replacement of the piperidine moiety with the different 6-membered rings resulted in a significant loss of binding affinity for 4C11 in the FACS analysis of compound **19–23** (MFI(**19**) = 11.44, MFI(**20**) = 12.84, MFI(**21**) = 12.47, in MFI (blank) = 11.34; MFI(**22**) = 26.67, MFI(**23**) = 20.21, in MFI(blank) = 26.79, data not shown), indicating a significant contribution from the piperidine ring which interacts with gp120 inducing conformational changes.

In view of their ability to induce conformational changes of gp120, the anti-HIV activity and cytotoxicity of the piperidine derivatives **13–18** were further evaluated, with the results shown in Table 2. The anti-HIV activity of the synthetic compounds was evaluated against various viral strains including both laboratory and primary isolates and IC_{50} and CC_{50} values were determined as those of compounds **4–6**. The *N*-methylpiperidine compound **13**, was not found to possess significant anti-HIV activity against a primary isolate, but was found to possess moderate anti-HIV activity against a laboratory isolate, a IIIB strain (IC_{50} = 67 μM). Anti-HIV activity was not observed however, even at concentrations of 100 μM of **13** against an 89.6 strain. The potency was approximately eight-fold lower than that of the parent compound **1** (IC_{50} = 8 μM), indicating a partial contribution of the hydrogen atom of the amino group of the piperidine ring to the bioactivity of CD4 mimic. Although compound **15**, with an *N*-isobutylpiperidine moiety, failed to show significant anti-HIV activity against laboratory isolates, relativity potent activity was observed against a primary isolate, an MTA strain (IC_{50} = 28 μM). Compounds **16** and **18**, which are *N*-acylpiperidines, were tested against laboratory isolates and significant anti-HIV activity was not observed even at 100 μM. Compounds **14** and **17**, with the carboxylic moieties, failed to show significant anti-HIV activity against laboratory isolates even at 100 μM, which are compatible with the FACS analysis. These results suggest that the N-substituent on the piperidine ring of CD4 mimic analogs may contribute to a critical interaction required for binding to gp120. Compounds **19–23** showed no significant anti-HIV activity against a IIIB strain even at 100 μM, which are compatible with the FACS analysis (data not shown).

All but one of the compounds **13–18** have no significant cytotoxicity to PM1/CCR5 cells ($CC_{50} \geqslant 260$ μM); the exception is compound **18** (CC_{50} = 45 μM). Compounds **13** and **15** show relatively potent anti-HIV activity without significant cytotoxicity.

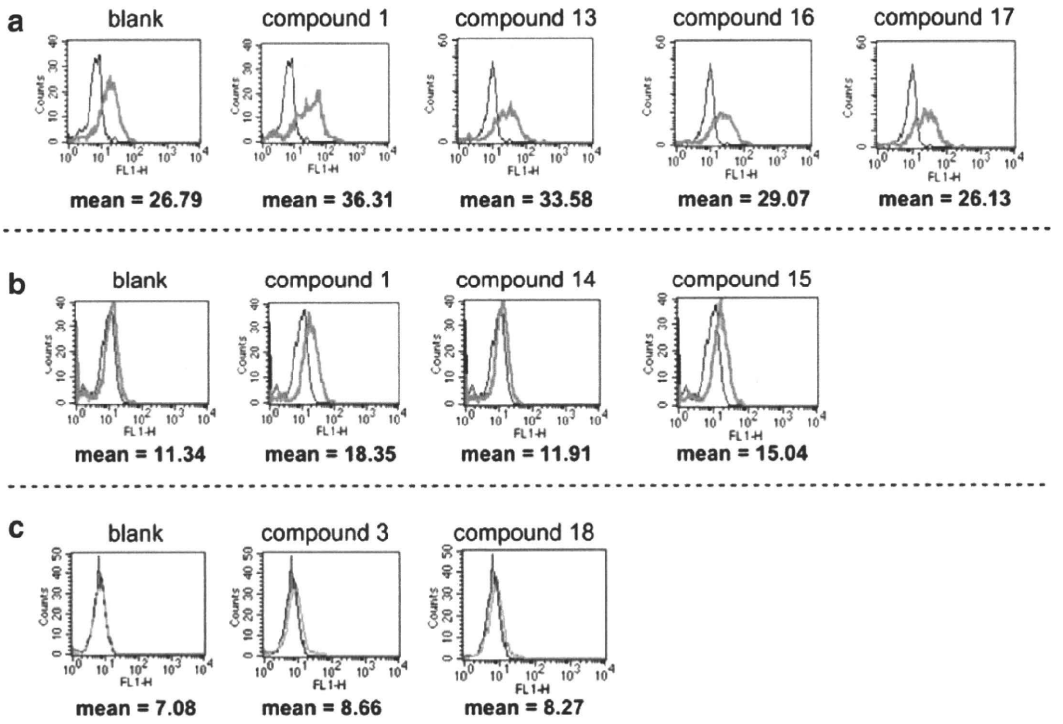

Figure 3. FACS analysis of compounds **1**, **3**, and **13–18**. The experimental procedures are described in Figure 2. The lanes of (a), (b) and (c) show independent experiments.

Table 2
Anti-HIV activity and cytotoxicity of compounds **13–18**[a]

Compd	R	IC_{50} (μM)			CC_{50} (μM)
		Laboratory isolates		Primary isolates	
		IIIB (X4)	89.6 (dual)	MTA (R5)	
1		8	10	ND	150
4	H	ND	ND	ND	100
13	Me	67	>100	ND	>300
14	CH_2CO_2H	>100	ND	ND	260
15	*i*Bu	>100	ND	28	>300
16	Ac	>100	>100	ND	>300
17	$C(O)CH_2CH_2CO_2H$	>100	>100	ND	>300
18	C(O)*i*Pr	>100	ND	ND	45

[a] All data with standard deviation are the mean values for at least three independent experiments.

The results for **15** showed it to have 3–6 times less cytotoxicity than **4** and **18**. This observation indicates that the alkylation of the piperidine nitrogen may be favorable because it lowers the cytotoxicity of CD4 mimic analogs.

In the course of the SAR studies on CD4 mimic analogs, we have already found that a CD4 mimic or sCD4 exhibited a remarkable synergistic effect[4e] with a 14-mer peptide CXCR4 antagonist T140.[9] This result indicates that the interaction of CD4 mimic with gp120 could facilitate the approach of CXCR4 to gp120 by exposing the co-receptor binding site of gp120. It was thought that the CD4 mimic analogs conjugated with a selective CXCR4 antagonist might as a consequence show a higher synergistic effect for the improvement of anti-HIV activity. In this context, efforts were made to synthesize and bioevaluate hybrid molecules that combined a CD4 mimic analog with 4F-benzoyl-TZ14011, which is a derivative of T140 optimized for CXCR4 binding and stability in vivo.[10]

The synthesis of hybrid molecules **27–29** is outlined in Scheme 4. To examine the influence of the linker length on anti-HIV activity and cytotoxicity, three hybrid molecules with linkers of different lengths were designed. Based on the fact that alkylation of the piperidine nitrogen, having no deleterious effects on bioactivity, is an acceptable modification of CD4 mimic analogs, the alkylamine moiety was incorporated into the nitrogen atom of the piperidine moiety to conjugate CD4 mimic analogs with 4F-benzoyl-TZ14011. Reductive alkylation of **4** with N^{α}-Boc-pyrrolidin-2-ol **24**, which exists in equilibrium with the corresponding aldehyde, and successive treatment with TFA and HCl/dioxane provided the amine hydrochloride **25**. Treatment of **25** with succinic anhydride under basic condition gave the corresponding acid **26**, which was subjected to condensation with the side chain of D-Lys[8] of 4F-benzoyl-TZ14011 in an EDC–HOBt system to give the desired hybrid molecule **27** with a tetramethylene linker.[11] Other hybrid molecules **28** and **29** bearing hexa- and octamethylene linkers, respectively, were prepared using the corresponding aldehydes **30** and **31**.

The assay results for these hybrid molecules **27–29** are shown in Table 3. To investigate the effect of conjugation of two molecules on binding activity against CXCR4, the inhibitory potency against

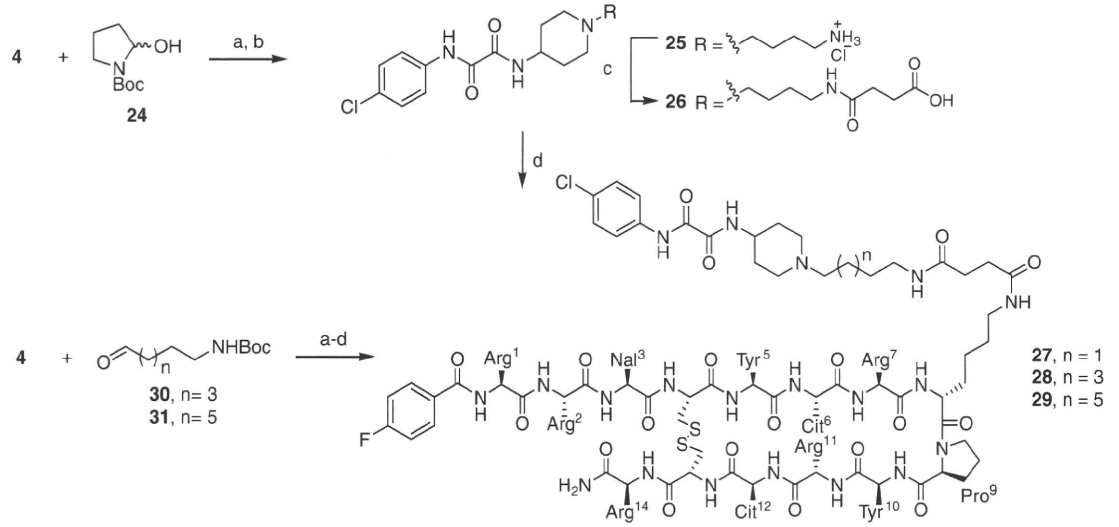

Scheme 4. Synthesis of hybrid molecules **27–29**. Reagents and conditions: (a) $NaBH(OAc)_3$, AcOH, DCE; (b) TFA, then 4 M HCl/1,4-dioxane; (c) succinic anhydride, pyridine, DMF, then 4 M HCl/1,4-dioxane; (d) 4F-benzoyl-TZ14011, EDC·HCl, HOBt·H_2O, Et_3N, DMF. Nal = L-3-(2-naphthyl)alanine, Cit = L-citrulline.

Table 3
CXCR4-binding activity, anti-HIV activity and cytotoxicity of hybrid molecules **27–29**[a]

Compd	EC_{50}[b] (μM)	IC_{50}[c] (μM)	CC_{50}[d] (μM)	SI (CC_{50}/IC_{50})
4F-benzoyl-TZ14011	0.0059	0.0131	ND	ND
1 (NBD-556)	ND	0 2.10	ND	19.2[e]
27 (C4)	0.0044	0.0509	8.60	169
28 (C6)	0.0187	0.0365	8.00	219
29 (C8)	0.0071	0.0353	8.60	244
AZT	ND	0.0493	ND	ND

[a] All data with standard deviation are the mean values for at least three independent experiments.
[b] EC_{50} values are based on the inhibition of [^{125}I]-SDF-1α binding to CXCR4 transfectants of CHO cells.
[c] IC_{50} values are based on the inhibition of HIV-1-induced cytopathogenicity in MT-2 cells.
[d] CC_{50} values are based on the reduction of the viability of mock-infected MT-2 cells.
[e] This value is based on the CC_{50} and IC_{50} values from Table 1.

binding of [^{125}I]-SDF-1α to CXCR4 was measured. All the hybrid molecules **27–29** significantly inhibited the SDF-1α binding to CXCR4. The corresponding EC_{50} values are: EC_{50}(**27**) = 0.0044 μM; EC_{50}(**28**) = 0.0187 μM; EC_{50}(**29**) = 0.0071 μM. These potencies are comparable to that of 4F-benzoyl-TZ14011 (EC_{50} = 0.0059 μM), indicating that introduction of the CD4 mimic analog into the D-Lys[8] residue of 4F-benzoyl-TZ14011 does not affect binding activity against CXCR4. Comparison of the binding activities of **27–29** showed that all hybrid molecules were essentially equipotent in inhibition of the binding of SDF-1α to CXCR4. This observation indicates that the linker length between two molecules has no effect on the binding inhibition.

Anti-HIV activity based on the inhibition of HIV-1 entry into the target cells was examined by the MTT assay using a IIIB(X4) strain. In this assay, the IC_{50} value of 4F-benzoyl-TZ14011 was 0.0131 μM. All hybrid molecules **27–29** showed significant anti-HIV activity [IC_{50}(**27**) = 0.0509 μM; IC_{50}(**28**) = 0.0365 μM; IC_{50}(**29**) = 0.0353 μM]; however, the potency was 2- to 4-fold lower than that of the parent compound 4F-benzoyl-TZ14011, indicating that the conjugation of CD4 mimic with a CXCR4 antagonist did not provide a significant synergistic effect. In view of the fact that the combinational uses of CD4 mimic with T140 produced a highly remarkable synergistic effect, the lower potency of hybrid molecules may be attributed to the inadequacy in the structure and/or the characters of the linkers. All the hybrid molecules **27–29** have relatively strong cytotoxicity [CC_{50}(**27**) = 8.6 μM; CC_{50}(**28**) = 8.0 μM; CC_{50}(**29**) = 8.6 μM]. However, selectivity indexes (SI = CC_{50}/IC_{50}) were 169 for **27**, 219 for **28**, and 244 for **29**, all 9–13 times higher than that of **1** (SI = 9.2). This result indicates that conjugation of a CD4 mimic analog with a selective CXCR4 antagonist can improve the SI of CD4 mimic.

The SAR study of a series of CD4 mimic analogs was conducted to investigate the contribution of the piperidine moiety of **1** to anti-HIV activity, cytotoxicity, and CD4 mimicry on conformational changes of gp120. The results indicate that (i) the methyl groups on the piperidine ring of **1** have no great influence on the activities of CD4 mimic; (ii) the presence of piperidine moiety is important for the CD4 mimicry; and (iii) N-substituents of the piperidine moiety contribute significantly to anti-HIV activity and cytotoxicity, as observed with N-alkyl groups such as methyl and isobutyl groups which show moderate anti-HIV activity and lower cytotoxicity.

Several hybrid molecules based on conjugation of a CD4 mimic with a selective CXCR4 antagonist were also synthesized and bioevaluated. All the hybrid molecules showed significant binding activity against CXCR4 comparable to the parent antagonist and exhibited potent anti-HIV activity. Although no significant synergistic effect was observed, conjugation of a CD4 mimic with a selective CXCR4 antagonist might lead to the development of novel type of CD4 mimic-based HIV-1 entry inhibitors, which possess higher selective indexes than a simple CD4 mimic. These results will be useful for the rational design and synthesis of a new type of HIV-1 entry inhibitors. Further structural modification studies of CD4 mimic are the subject of an ongoing project.

Acknowledgements

This work was supported by Grant-in-Aid for Scientific Research from the Ministry of Education, Culture, Sports, Science, and Technology of Japan, Japan Human Science Foundation, and Health and Labour Sciences Research Grants from Japanese Ministry of Health, Labor, and Welfare. T.T. and N.O. are grateful for the JSPS Reseach Fellowships for Young Scientist.

References and notes

1. Chan, D. C.; Kim, P. S. *Cell* **1998**, *93*, 681.
2. (a) Alkhatib, G.; Combadiere, C.; Broder, C. C.; Feng, Y.; Kennedy, P. E.; Murphy, P. M.; Berger, E. A. *Science* **1996**, *272*, 1955; (b) Choe, H.; Farzan, M.; Sun, Y.; Sullivan, N.; Rollins, B.; Ponath, P. D.; Wu, L.; Mackay, C. R.; LaRosa, G.; Newman, W.; Gerard, N.; Gerard, C.; Sodroski, J. *Cell* **1996**, *85*, 1135; (c) Deng, H. K.; Liu, R.; Ellmeier, W.; Choe, S.; Unutmaz, D.; Burkhart, M.; Marzio, P. D.; Marmon, S.; Sutton, R. E.; Hill, C. M.; Davis, C. B.; Peiper, S. C.; Schall, T. J.; Littman, D. R.; Landau, N. R. *Nature* **1996**, *381*, 661; (d) Doranz, B. J.; Rucker, J.; Yi, Y. J.; Smyth, R. J.; Samson, M.; Peiper, S. C.; Parmentier, M.; Collman, R. G.; Doms, R. W. *Cell* **1996**, *85*, 1149; (e) Dragic, T.; Litwin, V.; Allaway, G. P.; Martin, S. R.; Huang, Y.; Nagashima, K. A.; Cayanan, C.; Maddon, P. J.; Koup, R. A.; Moore, J. P.; Paxton, W. A. *Nature* **1996**, *381*, 667.
3. Feng, Y.; Broder, C. C.; Kennedy, P. E.; Berger, E. A. *Science* **1996**, *272*, 872.
4. (a) Zhao, Q.; Ma, L.; Jiang, S.; Lu, H.; Liu, S.; He, Y.; Strick, N.; Neamati, N.; Debnath, A. K. *Virology* **2005**, *339*, 213; (b) Schön, A.; Madani, N.; Klein, J. C.; Hubicki, A.; Ng, D.; Yang, X.; Smith, A. B., III; Sodroski, J.; Freire, E. *Biochemistry* **2006**, *45*, 10973; (c) Madani, N.; Schön, A.; Princiotto, A. M.; LaLonde, J. M.; Courter, J. R.; Soeta, T.; Ng, D.; Wang, L.; Brower, E. T.; Xiang, S.-H.; Do Kwon, Y.; Huang, C.-C.; Wyatt, R.; Kwong, P. D.; Freire, E.; Smith, A. B., III; Sodroski, J. *Structure* **2008**, *16*, 1689; (d) Haim, H.; Si, Z.; Madani, N.; Wang, L.; Courter, J. R.; Princiotto, A.; Kassa, A.; DeGrace, M.; McGee-Estrada, K.; Mefford, M.; Gabuzda, D., ; Smith, A. B., III; Sodroski, J. *ProS Pathogens* **2009**, *5*, 1; (e) Yamada, Y.; Ochiai, C.; Yoshimura, K.; Tanaka, T.; Ohashi, N.; Narumi, T.; Nomura, W.; Harada, S.; Matsushita, S.; Tamamura, H. *Bioorg. Med. Chem. Lett.* **2010**, *20*, 354; (f) Yoshimura, K.; Harada, S.; Shibata, J.; Hatada, M.; Yamada, Y.; Ochiai, C.; Tamamura, H.; Matsushita, S. *J. Virol.* **2010**, *84*, 7558.
5. Protein Data Bank (PDB) (entry 1RZJ).
6. Olofson, R. A.; Abbott, D. E. *J. Org. Chem.* **1984**, *49*, 2795.
7. The synthesis of compound **4**: To the solution of compound **10** (104 mg, 0.52 mmol) in dry THF (4.0 mL), Et_3N (159 μL, 1.15 mmol), HOBt·H_2O (87 mg, 0.57 mmol), EDCI·HCl (109 mg, 0.57 mmol) and 4-amino-1-benzylpiperidine (109 μL, 0.57 mmol) were added with stirring at 0 °C, and continuously stirred for 6 h with warming to room temperature under N_2 atmosphere. After concentration under reduced pressure, the residue was extracted with EtOAc. The extract was washed with aq saturated $NaHCO_3$ and brine, and dried over $MgSO_4$. Concentration under reduced pressure followed by flash chromatography over silica gel with $CHCl_3$–MeOH (20:1) including 1% Et_3N gave the crude benzyl amine as a white powder. To the solution of the above crude benzyl amine (95 mg, 0.26 mmol) in dry CH_2Cl_2 (10 mL), 1-chloroethyl chloroformate (110 μL, 0.68 mmol) was added dropwise with stirring at 0 °C. The mixture was then refluxed for 3 h under N_2 atmosphere. After concentration under reduced pressure, the residue was resolved in MeOH (10 mL) and then refluxed for 1 h. Concentration under reduced pressure gave a crude product. Reprecipitation with MeOH–Et_2O afforded a white powder of the title compound **4** (33 mg, 46% yield). δ_H(400 MHz; CD_3OD) 1.83–1.92 (2H, m, CH_2), 2.10–2.17 (2H, m, CH_2), 3.13 (2H, t, *J* 12.5, CH_2), 3.34 (1H, m, NH), 3.42–3.49 (1H, m, CH_2), 4.04 (1H, m, CH), 7.34 (2H, m, ArH), 7.51 (1H, m, NH), 7.73 (2H, m, ArH), 8.84 (1H, m, NH); LRMS (ESI), *m/z* calcd for $C_{13}H_{17}ClN_3O_2$ $(MH)^+$ 282.10, found 282.14.
8. Yoshimura, K.; Shibata, J.; Kimura, T.; Honda, A.; Maeda, Y.; Koito, A.; Murakami, T.; Mitsuya, H.; Matsushita, S. *AIDS* **2006**, *20*, 2065.
9. (a) Tamamura, H.; Xu, Y.; Hattori, T.; Zhang, X.; Arakaki, R.; Kanbara, K.; Omagari, A.; Otaka, A.; Ibuka, T.; Yamamoto, N.; Nakashima, H.; Fujii, N. *Biochem. Biophys. Res. Commun.* **1998**, *253*, 877; (b) Tamamura, H.; Hiramatsu, K.; Mizumoto, M.; Ueda, S.; Kusano, S.; Terakubo, S.; Akamatsu, M.; Yamamoto, N.; Trent, J. O.; Wang, Z.; Peiper, S. C.; Nakashima, H.; Otaka, A.; Fujii, N. *Org. Biomol. Chem.* **2003**, *1*, 3663.
10. Hanaoka, H.; Mukai, T.; Tamamura, H.; Mori, T.; Ishino, S.; Ogawa, K.; Iida, Y.; Doi, R.; Fujii, N.; Saji, H. *Nucl. Med. Biol.* **2006**, *33*, 489.
11. The synthesis of a hybrid molecule **27**: To the solution of compound **26** (2.6 mg, 4.6 μmol) in DMF (1.0 mL), Et_3N (26 μL, 92 μmol), HOBt·H_2O (3.5 mg, 23 μmol) and EDCI·HCl (4.5 mg, 23 μmol) were added with stirring at 0 °C, and stirred for 1 h at room temperature. To the mixture 4F-benzoyl-TZ14011 (15 mg, 4.1 μmol) was then added and the mixture was stirred for 24 h at room temperature under N_2 atmosphere. After concentration under reduced pressure, the residue was purified by reversed phase HPLC (t_R = 23 min, elution: a linear gradient of 27–31% acetonitrile containing 0.1% TFA over 30 min) to afford a fluffy white powder of the desired compound **27** (1.3 mg, 9.8%). LRMS (ESI), *m/z* 2621.20 $[M+H]^+$, calcd 2620.25.

JOURNAL OF VIROLOGY, Aug. 2010, p. 7558–7568 Vol. 84, No. 15
0022-538X/10/$12.00 doi:10.1128/JVI.00227-10

Enhanced Exposure of Human Immunodeficiency Virus Type 1 Primary Isolate Neutralization Epitopes through Binding of CD4 Mimetic Compounds[▽]

Kazuhisa Yoshimura,[1] Shigeyoshi Harada,[1] Junji Shibata,[1] Makiko Hatada,[1] Yuko Yamada,[2] Chihiro Ochiai,[2] Hirokazu Tamamura,[2] and Shuzo Matsushita[1]*

Division of Clinical Retrovirology and Infectious Diseases, Center for AIDS Research, Kumamoto University, Kumamoto, Japan,[1] and Institute of Biomaterials and Bioengineering, Tokyo Medical and Dental University, Chiyoda-ku, Tokyo, Japan[2]

Received 17 March 2010/Accepted 13 May 2010

***N*-(4-Chlorophenyl)-*N'*-(2,2,6,6-tetramethyl-piperidin-4-yl)-oxalamide (NBD-556) is a low-molecular-weight compound that reportedly blocks the interaction between human immunodeficiency virus type 1 (HIV-1) gp120 and its receptor CD4. We investigated whether the enhancement of binding of anti-gp120 monoclonal antibodies (MAbs) toward envelope (Env) protein with NBD-556 are similar to those of soluble CD4 (sCD4) by comparing the binding profiles of the individual MAbs to Env-expressing cell surfaces. In flow cytometric analyses, the binding profiles of anti-CD4-induced epitope (CD4i) MAbs toward NBD-556-pretreated Env-expressing cell surfaces were similar to the binding profiles toward sCD4-pretreated cell surfaces. To investigate the binding position of NBD-556 on gp120, we induced HIV-1 variants that were resistant to NBD-556 and sCD4 *in vitro*. At passage 21 in the presence of 50 μM NBD-556, two amino acid substitutions (S375N in C3 and A433T in C4) were identified. On the other hand, in the selection with sCD4, seven mutations (E211G, P212L, V255E, N280K, S375N, G380R, and G431E) appeared during the passages. The profiles of the mutations after the selections with NBD-556 and sCD4 were very similar in their three-dimensional positions. Moreover, combinations of NBD-556 with anti-gp120 MAbs showed highly synergistic interactions against HIV-1. We further found that after enhancing the neutralizing activity by adding NBD-556, the contemporaneous virus became highly sensitive to antibodies in the patient's plasma. These findings suggest that small compounds such as NBDs may enhance the neutralizing activities of CD4i and anti-V3 antibodies *in vivo*.**

Human immunodeficiency virus type 1 (HIV-1) replicates continuously in the face of a strong antibody (Ab) response, although Abs effectively control many viral infections (3). Neutralizing Abs (NAbs) are directed against the HIV-1 envelope (Env) protein, which is a heterodimer comprising an extensively glycosylated CD4-binding subunit (gp120) and an associated transmembrane protein (gp41). Env proteins are present on the virion surface as "spikes" composed of trimers of three gp120-gp41 complexes (20, 21, 29). These spikes resist neutralization through epitope occlusion within the oligomer, extensive glycosylation, extension of variable loops from the surface of the complex, and steric and conformational blocking of receptor binding sites (16, 18, 20).

Ab access to conserved regions is further limited because viral entry is a stepwise process involving conformational changes that lead to only transient exposure of conserved domains such as the coreceptor binding site (4, 5). However, some early strains of HIV-1 appear to be highly susceptible to neutralization by Abs (1, 10). For instance, subtype A HIV-1 envelopes from the early stage of infection exhibit a broad range of neutralization sensitivities to both autologous and heterologous plasma (1), suggesting that at least a subset of the envelopes have some preserved and/or exposed neutralization epitopes. It is well known that the potential for neutralizing properties of particular Abs is enhanced after binding of soluble CD4 (sCD4), especially NAbs against CD4-induced epitopes (CD4i Abs) (27) and some anti-V3 Abs (22). CD4i Abs are detected in plasma samples from many patients at an early stage of HIV-1 infection (9). Consequently, we hypothesize that small compounds such as sCD4 can enhance the neutralizing activities of CD4i Abs and some anti-V3 Abs not only *in vitro* but also *in vivo*.

In a previous report, two low-molecular-weight compounds that presumably interfere with viral entry of HIV-1 into cells were described (35). These two *N*-phenyl-*N'*-(2,2,6,6-tetramethyl-piperidin-4-yl)-oxalamide analogs, NBD-556 and NBD-557, comprise a novel class of HIV-1 entry inhibitors that block the interaction between gp120 and CD4. These compounds were found to be equally potent inhibitors of both X4 and R5 viruses in CXCR4- and CCR5-expressing cell lines, respectively (35). Schön et al. (25) also reported that NBD-556 binds to gp120 in a process characterized by a large favorable change in enthalpy that is partially compensated for by a large unfavorable entropy change, representing a thermodynamic signature similar to that observed for binding of sCD4 to gp120. In a recent study, Madani et al. (23) reported the following findings: (i) NBD-556 binds within the Phe43 cavity, a highly conserved and functionally important pocket formed as gp120 assumes the CD4-bound conformation; (ii) the NBD-556 phenyl ring projects into the Phe43 cavity; (iii) the enhancement of CD4-independent infection by NBD-556 requires the induction of conformational changes in gp120; and (iv) increased

* Corresponding author. Mailing address: Division of Clinical Retrovirology and Infectious Diseases, Center for AIDS Research, Kumamoto University, Kumamoto 860-0811, Japan. Phone: 81-96-373-6536. Fax: 81-96-373-6537. E-mail: shuzo@kumamoto-u.ac.jp.

[▽] Published ahead of print on 26 May 2010.

affinities of NBD-556 analogs toward gp120 improve the antiviral potency during infection of CD4-expressing cells. The latter two studies demonstrated that low-molecular-weight compounds such as NBDs can induce conformational changes in the HIV-1 gp120 glycoprotein similar to those observed upon sCD4 binding (23, 25). The authors of these studies concluded that their data supported the importance of gp120 residues near the Phe43 cavity in binding to NBD-556 and lent credence to the docked binding mode.

In the present study, we investigated the binding position of NBD-556 on gp120 by inducing HIV-1 variants that were resistant to NBD-556 by exposing HIV-1_{IIIB} to increasing concentrations of the compound *in vitro*. We also induced sCD4-resistant HIV-1_{IIIB} variants and compared the profile of the sCD4-resistant mutations to that of the NBD-556-resistant mutations. We subsequently examined the virological properties of pseudotyped HIV-1 clones carrying the NBD-556 and sCD4 resistance-associated *env* gene mutations. Our findings provide a foundation for understanding the interaction of NBD-556 with the CD4-binding site of HIV-1 gp120. We also evaluated the anti-HIV-1 interactions between plasma NAbs and NBD-556 *in vitro* and considered the possibility of using the data as a key to opening the shield covering the conserved epitopes targeted by NAbs.

(This study was presented in part at the 15th Conference on Retroviruses and Opportunistic Infection, Boston, MA, 3 to 6 February 2008 [Abstract 736].)

MATERIALS AND METHODS

Cells, culture conditions, and reagents. The CD4-positive T-cell line PM1 was maintained in RPMI 1640 (Sigma, St. Louis, MO) supplemented with 10% heat-inactivated fetal calf serum (FCS; HyClone Laboratories, Logan, UT), 50 U of penicillin/ml, and 50 μg of streptomycin/ml. PM1/CCR5 cells were generated by standard retrovirus-mediated transduction of PM1 cells with pBABE-CCR5 provided by the National Institutes of Health AIDS Research and Preference Reagent Program (NIH ARRRP) (24, 34). PM1/CCR5 cells were maintained in RPMI 1640 supplemented with 10% heat-inactivated FCS, 50 U of penicillin/ml, 50 μg of streptomycin/ml, and 0.1 mg of G418 (Invitrogen, Carlsbad, CA)/ml. The TZM-bl cell line was obtained from the NIH ARRRP and maintained in Dulbecco modified Eagle medium (Sigma) supplemented with 10% FCS.

NBD-556 (molecular weight, 337.84) and YYA-004 (molecular weight, 303.4), which has the same structure as JRC-I-300 (23), were synthesized as previously described (23, 25, 30). KD-247 (12), 3E4, and 0.5γ (unpublished) are anti-gp120-V3 monoclonal Abs (MAbs). 17b (27), 4C11, and 4E9C (unpublished) are MAbs against CD4-induced epitopes (CD4i Abs). 17b, 2G12 (a MAb against the gp120 glycan), and b12 (a MAb against the CD4-binding site [CD4bs] epitope) were provided by the NIH ARRRP. The 0.5δ antibody established in our laboratory is an anti-CD4bs MAb (unpublished results). RPA-T4 (an anti-CD4 MAb) was purchased from BD Biosciences Pharmingen (San Jose, CA). Recombinant human sCD4 was purchased from R&D Systems, Inc. (Minneapolis, MN).

MAbs 3E4, 0.5γ, 0.5δ, 4C11, and 4E9C were human MAbs established from a patient with long-term nonprogressive illness. B cells from the patient's peripheral blood mononuclear cells (PBMC) were transformed by Epstein-Barr virus, followed by cloning. Culture supernatant from an individual clone was screened for reactivity to $gp120_{SF2}$ by enzyme-linked immunosorbent assay (ELISA). The specificity of the antibodies was determined by gp120 capture ELISA and fluorescence-activated cell sorting analysis of HIV-1_{JR-FL}-infected PM1 cells in the presence or absence of sCD4. The binding specificity was further assessed by an ELISA using peptides corresponding to the V3 sequence of various isolates. Based on these binding data, we classified them as follows: V3 MAbs, 3E4 and 0.5γ; CD4bs MAb, 0.5δ; and CD4i MAbs, 4C11 and 4E9C.

The laboratory-adapted HIV-1 strains HIV-$1_{89.6}$, HIV-1_{BaL}, HIV-1_{SF162}, HIV-1_{JR-FL}, and HIV-1_{YU2} were propagated in phytohemagglutinin-activated PBMC. These viruses were then passaged in PM1/CCR5 cells, and the culture supernatants were stored at −150°C prior to use. R5 primary HIV-1 isolates (HIV-$1_{Pt.1}$, HIV-$1_{Pt.2}$, HIV-$1_{Pt.3}$, and HIV-$1_{Pt.4}$) were isolated from four Japanese patients in our laboratory. All patients were at a stage of chronic infection. HIV-$1_{Pt.1}$, HIV-$1_{Pt.3}$, and HIV-$1_{Pt.4}$ were isolated from drug-naive patients, and HIV-$1_{Pt.2}$ was isolated from a drug-experienced patient and passaged in phytohemagglutinin-activated PBMC. Infected PBMC were cocultured with PM1/CCR5 cells for 4 to 5 days, and the culture supernatants were stored at −150°C until used. Nucleotide sequences of the gp120 from the four primary isolates were deposited in the DNA Data Bank of Japan under accession numbers AB553911 to AB553914.

Susceptibility assay. The sensitivities of six laboratory-adapted viruses, four primary isolates, and HIV-1_{IIIB} viruses passaged in the presence of sCD4 or NBD-556 were determined by the MTT [3-(4,5-dimethylthiazol-2-yl)-2,5-diphenyltetrazolium bromide] assay as previously described with minor modifications (31). Briefly, PM1/CCR5 cells (2×10^3 cells/well) were exposed to 100 times the 50% tissue culture infective dose ($TCID_{50}$) of the viruses in the presence of various concentrations of sCD4 or NBD-556 in 96-well round-bottom microculture plates, followed by incubation at 37°C for 7 days. After removal of 100 μl of the medium, 10 μl of MTT solution (7.5 mg/ml) in phosphate-buffered saline (PBS) was added to each well. The plate was then incubated at 37°C for 3 h. Subsequently, the produced formazan crystals were dissolved by adding 100 μl of acidified isopropanol containing 4% (vol/vol) Triton X-100 to each well. The optical densities at a wavelength of 570 nm were measured in a microplate reader. All assays were performed in duplicate or triplicate. We also determined the concentration for 50% cytotoxicity (CC_{50}) by using the MTT assay.

The sensitivities of the HIV-$1_{Pt.3}$ primary isolate to KD-247 (anti-V3 MAb), 4E9C (CD4i MAb), and autologous plasma IgG in the presence or absence of NBD-556 were also determined by using the MTT assay. To exclude any influence of plasma factors, such as antiviral drugs, cytokines, and chemokines, on the neutralization activities, we used IgG from the patient's plasma, which was purified using protein A-Sepharose (Affi-gel Protein A; Bio-Rad, Hercules, CA) (19).

Flow cytometric analysis. HIV-1_{JR-FL} chronically infected PM1 cells were preincubated with or without sCD4 (0.5 μg/ml) and NBD-556 (1, 3, 10, 30, 90, and 100 μM) for 15 min and then incubated with various anti-HIV-1 MAbs (17b, 4C11, KD-247, 3E4, and 0.5γ) at 4°C for 30 min. The cells were washed with PBS, and a fluorescein isothiocyanate-conjugated goat anti-human IgG Ab was used for Ab detection. Flow cytometry was performed with a FACSCalibur flow cytometer (BD Biosciences), and the data were analyzed by using the BD CellQuest version 3.1 software (BD Biosciences).

Data analysis and evaluation of synergy. Analyses of the synergistic, additive, and antagonistic effects of the antiviral agents were initially performed according to the median effect principle using the CalcuSyn version 2 computer program (6) to provide estimates of the 50% inhibitory concentration (IC_{50}) values of the antiviral agents in combination. Combination indices (CIs) were estimated from the data and reflected the nature of the interactions between KD-247 and sCD4 or NBD-556 and between NBD-556 and CD4i MAb 4C11 or anti-CD4bs MAb 0.5δ against HIV-1_{JR-FL} or HIV-1_{IIIB} on PM1/CCR5 cells as determined by the MTT assay. A CI of <0.9 indicated synergy, a CI between 0.9 and 1.1 indicated additivity, and a CI of >1.1 indicated antagonism. The CI value was directly proportional to the amount of synergy for the combination regimen. For example, values of <0.5 represented a high degree of synergy, while values of >1.5 represented significant antagonism. This approach has been widely used in analyses of antiviral interactions and was chosen to allow comparability with published literature.

Docking simulation. The structure for NBD-556 was built in SYBYL 7.1 (Tripos, St. Louis, MO) and minimized with the MMFF94 force field and partial charges (15). Using FlexSIS through its SYBYL module, docking of NBD-556 was performed into the crystal structure of gp120 obtained from the Protein Data Bank (PDB; entry 1RZJ). The binding site was defined as residues Val255, Asp368, Glu370, Ser375, Ile424, Trp427, Val430, and Val475, including residues located within a radius of 4.4 Å. The structure of the ligand was treated flexibly, and all other options were set to their default values. Figures were generated using SwissPdb Viewer version 3.9 (SPdbViewer) (13) and ViewerLite version 5.0 (Accelrys, Inc., San Diego, CA). We also generated a simian immunodeficiency virus (SIV) gp120 figure (PDB entry 2BF1) to compare the sites of the mutations in HIV-1 gp120 using the same software programs.

Isolation of NBD-556- and sCD4-resistant mutants from HIV-1_{IIIB} *in vitro*. To select NBD-556 and sCD4 escape viruses, HIV-1_{IIIB} was treated with various concentrations of NBD-556 or sCD4 and then infected into PM1/CCR5 cells as previously described with minor modifications (32). Viral replication was monitored by observation of any cytopathic effects in PM1/CCR5 cells. The culture supernatants were harvested on day 7 and used to infect fresh PM1/

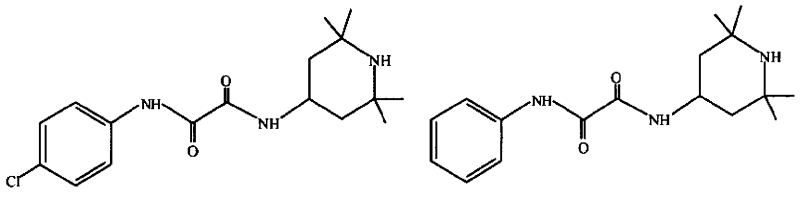

NBD-556 **YYA-004**

FIG. 1. Structures of NBD-556 and YYA-004.

CCR5 cells for the next round of culture in the presence of increasing concentrations of NBD-556 or sCD4. When the viruses began to propagate in the presence of NBD-556 or sCD4, the concentration was further increased. After the viruses were passaged using up to 50 μM NBD-556 or 20 μg of sCD4/ml in PM1/CCR5 cells, the resulting viruses, designated NBD-556(20)14p, NBD-556(50)17p, and sCD4(20)5p, were recovered from the passaged cell culture supernatants.

Proviral DNA extracts from cells cultured with several concentrations of NBD-556 and sCD4 were subjected to PCR amplification using *Taq* polymerase (Takara, Shiga, Japan). The amplified products were cloned into pCR2.1 (Invitrogen), and the *env* regions in both the passaged and selected viruses were sequenced by using an ABI Prism 3110 automated DNA sequencer (ABI, Foster City, CA).

Construction of mutant Env expression vectors. Proviral DNA was extracted from the passaged HIV-1_{IIIB}-infected PM1/CCR5 cells by using a QIAamp DNA blood minikit (Qiagen, Valencia, CA). For the construction of Env expression vectors, we used pCXN2, which contains a chicken actin promoter. Briefly, we amplified the passaged HIV-1_{IIIB} gp160 regions using LA *Taq* (Takara) with the primers ENVA (5′-GGCTTAGGCATCTCCTATGGCAGGAAGAA-3′) and ENVN (5′-CTGCCAATCAGGGAAGTAGCCTTGTGT-3′). The PCR products were inserted into pCR-XL-TOPO (Invitrogen). The EcoRI fragment of pCR-XL-IIIB containing the entire *env* region was ligated into pCXN2 to give pCXN-IIIBwt. pCXN-IIIB(S375N), pCXN-IIIB(V255E), and pCXN-IIIB(A433T) were generated by site-directed mutagenesis using a QuikChange site-directed mutagenesis kit (Stratagene, La Jolla, CA) in accordance with the manufacturer's instructions with the primer pairs S375Nfw (5′-AAATTGTAAC GCACAATTTTAATTGTGGAGG-3′) and S375Nrv (5′-CCTCCACAATTAA AATTGTGCGTTACAATTT-3′), V255Efw (5′-GAATTAGGCCAGTAGAAT CAACTCAACTGCT-3′) and V255Erv (5′-AGCAGTTGAGTTGATTCTACT GGCCTAATTC-3′), and A433Tfw (5′-CAGGAAGTAGGAAAAACAATGTA TGCCCCTC-3′) and A433Trv (5′-GAGGGGCATACATTGTTTTTCCTACTT CCTG-3′), respectively.

Pseudovirus preparation. Portions, 5 μg of pSG3ΔEnv and 0.5 μg of pRSV-Rev (17), supplied by the NIH ARRRP, and a 4.5-μg portion of HIV-1_{IIIB} Env-expressing pCXN2 were cotransfected into 293T cells using the Effectene transfection reagent (Qiagen). At 48 h after transfection, the pseudovirus-containing supernatants were harvested, filtered through a 0.2-μm-pore-size filter, and stored at −80°C. The pseudovirus activities were measured with a luminescence assay using TZM-bl cells as previously described (28).

Single-round virus infection assay. A single-cycle infectivity assay was used to measure the neutralization of HIV-1_{IIIB} pseudoviruses as described previously (26, 28). Briefly, NBD-556, YYA-004, sCD4, 2G12, b12, RPA-T4, or 4C11 at various concentrations and a pseudovirus suspension corresponding to 100 $TCID_{50}$ were preincubated in the absence or presence of 1 μM NBD-556 for 15 min on ice. The virus-compound mixtures were added to TZM-bl cells, which had been seeded in a 96-well plate (1.5×10^4 cells/well) on the previous day. The cultures were incubated for 2 days at 37°C, washed with PBS, and lysed with lysis solution (Galacto-Star mammalian reporter gene assay system; ABI). After transfer of the cell lysates to luminometer plates, the β-galactosidase activity (in relative light units) in each well was measured by using 50-fold-diluted Galacto-Star substrate in a reaction buffer diluent (100 μl/well; ABI) in a TR717 microplate luminometer (ABI). The reduction in infectivity was determined by comparing the relative light units in the presence or absence of each compound and expressed as the percentage of neutralization. Each assay was repeated two to three times.

RESULTS

Anti-HIV-1 activities of sCD4, NBD-556, and YYA-004 for laboratory strains and primary HIV-1 isolates. Initially, we determined the inhibitory activities of sCD4, NBD-556, and YYA-004, which has a phenyl group instead of the *p*-chlorophenyl group of NBD-556 (Fig. 1), on the infection of PM1/CCR5 cells by different laboratory-adapted HIV-1 strains and different HIV-1 primary isolates of subtype B, including both X4 and R5 viruses, by using a previously reported method (33). sCD4 inhibited the laboratory-adapted HIV-1 strains HIV-1_{IIIB}, HIV-$1_{89.6}$, HIV-1_{BaL}, HIV-1_{SF162}, HIV-$1_{JR\text{-}FL}$, and HIV-1_{YU2} with IC_{50}s ranging from 0.26 to 6.1 μg/ml (Table 1). NBD-556 inhibited the X4 virus HIV-1_{IIIB} and dualtropic virus HIV-$1_{89.6}$ with IC_{50}s of 7.8 and 11.4 μM, respectively, but did not inhibit the R5 viruses HIV-1_{BaL}, HIV-1_{SF162}, HIV-$1_{JR\text{-}FL}$, and HIV-1_{YU2} with IC_{50}s of >30 μM. We also tested sCD4 and NBD-556 against the R5 primary isolates HIV-$1_{Pt.1}$, HIV-$1_{Pt.2}$, HIV-$1_{Pt.3}$, and HIV-$1_{Pt.4}$. sCD4 effectively inhibited all of the primary isolates at concentrations of 0.2 to 7.4 μg/ml. On the other hand, NBD-556 inhibited two of the four primary

TABLE 1. Inhibitory activities of sCD4 and NBD-556 toward infection by laboratory and primary strains of HIV-1

Virus	Subtype	Cell	Mean IC_{50}[a] ± SD		
			sCD4 (μg/ml)	NBD-556 (μM)	YYA-004 (μM)
Laboratory-adapted viruses					
X4					
HIV-1_{IIIB}	B	PM1/CCR5	0.26 ± 0.17	7.8 ± 2.6	>100
Dual					
HIV-$1_{89.6}$	B	PM1/CCR5	0.87 ± 0.09	11.4 ± 2.4	>100
R5					
HIV-1_{BaL}	B	PM1/CCR5	1.7 ± 0.28	>30	>100
HIV-1_{SF162}	B	PM1/CCR5	3.6 ± 0.64	>30	>100
HIV-$1_{JR\text{-}FL}$	B	PM1/CCR5	3.6 ± 0.71	>30	>100
HIV-1_{YU2}	B	PM1/CCR5	6.1 ± 2.00	>30	>100
Primary isolates					
R5					
HIV-$1_{Pt.1}$	B	PM1/CCR5	0.2 ± 0.04	3.6 ± 0.67	>100
HIV-$1_{Pt.2}$	B	PM1/CCR5	1.6 ± 0.21	>30	>100
HIV-$1_{Pt.3}$	B	PM1/CCR5	3.7 ± 0.42	11.8 ± 1.6	>100
HIV-$1_{Pt.4}$	B	PM1/CCR5	7.4 ± 1.30	>30	>100

[a] PM1/CCR5 cells (2×10^3) were exposed to 100 $TCID_{50}$ of each virus and then cultured in the presence of various concentrations of sCD4, NBD-556, or YYA-004 as indicated. The IC_{50}s were determined by using the MTT assay on day 7 of culture. All assays were conducted in duplicate, and the data shown represent the means derived from the results of two to three independent experiments. For NBD-556, CC_{50} = 140 μM; for YYA-004, CC_{50} = 350 μM. (The CC_{50} is the concentration for 50% cytotoxicity.)

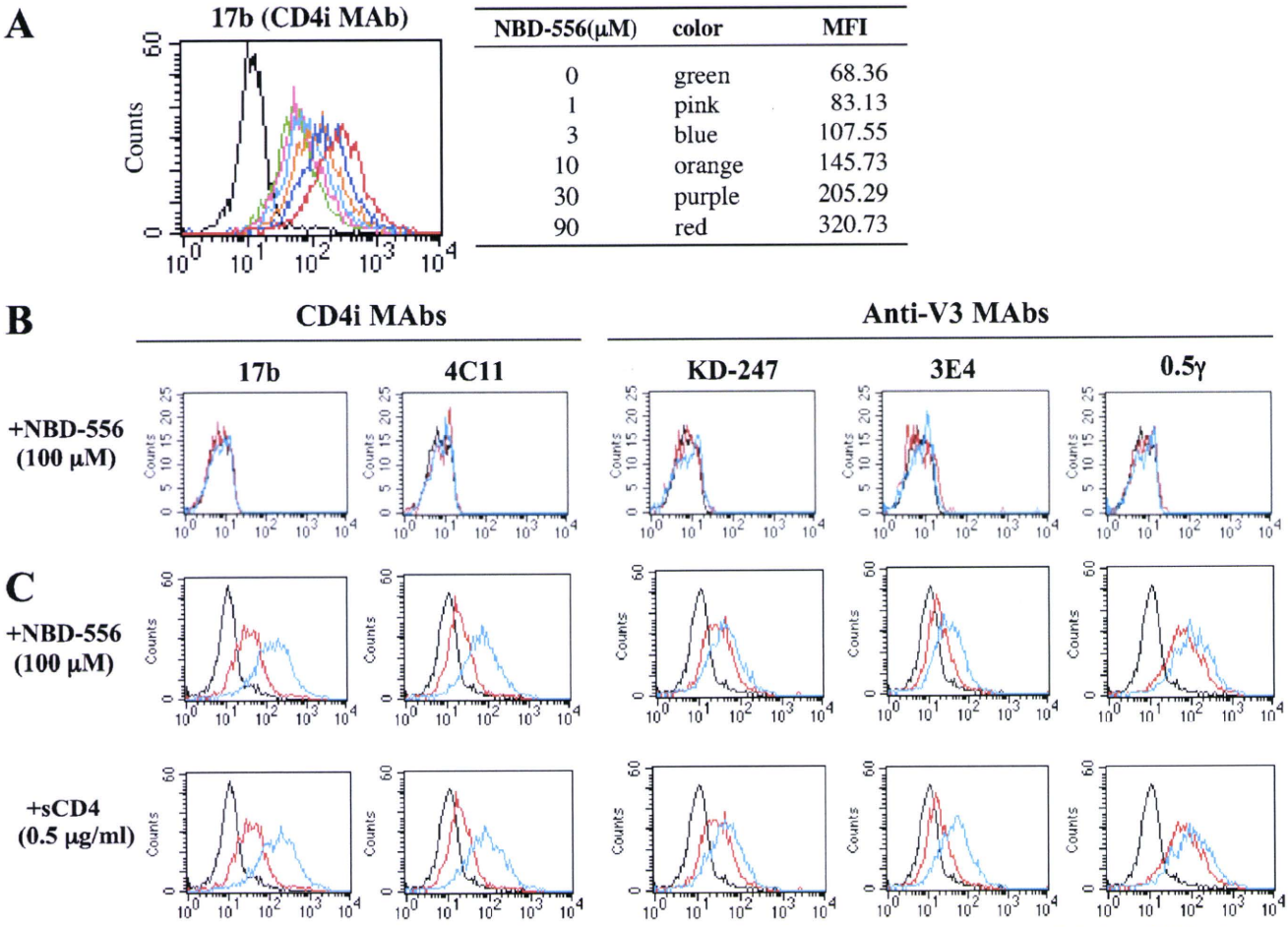

NBD-556(μM)	color	MFI
0	green	68.36
1	pink	83.13
3	blue	107.55
10	orange	145.73
30	purple	205.29
90	red	320.73

FIG. 2. Comparisons of MAb binding to cell surface-expressed gp120 with sCD4 and NBD-556. HIV-$1_{JR\text{-}FL}$ chronically infected PM1 cells were preincubated with or without NBD-556 (A, 1 to 90 μM; C, 100 μM) or sCD4 (C, 0.5 μg/ml), and uninfected PM1 cells were also preincubated with or without NBD-556 (B, 100 μM) for 15 min, and then incubated with various anti-HIV-1 MAbs (17b, 4C11, KD-247, 3E4, and 0.5γ) at 4°C for 30 min. The cells were washed, and a fluorescein isothiocyanate-conjugated anti-human IgG was used for detection. (A) Color lines show the concentrations of NBD-556: green, 0 μM; pink, 1 μM; blue, 3 μM; orange, 10 μM; purple, 30 μM; and red, 90 μM. (B and C) Red line shows no preincubated with NBD-556 or sCD4. Blue line shows preincubated with NBD-556 or sCD4. Black line shows using a control IgG MAb.

isolates, HIV-$1_{Pt.1}$ and HIV-$1_{Pt.3}$, with IC_{50}s of 3.6 and 11.8 μM, respectively (Table 1). YYA-004 did not show significant anti-HIV activity against any of the strains tested up to a concentration of 100 μM. The *in vitro* cytotoxicities of NBD-556 and YYA-004 toward PM1/CCR5 cells used for the anti-HIV-1 infectivity studies were determined by using the MTT assay. The CC_{50} values of NBD-556 and YYA-004 toward PM1/CCR5 cells were 140 and 350 μM, respectively (Table 1).

Comparison of Ab binding to cell surface-expressed HIV-$1_{JR\text{-}FL}$ Env with NBD-556 and sCD4. To compare the effect of NBD-556 with that of sCD4 with respect to the induction of conformational change in the trimeric gp120, the binding of CD4i MAbs (17b and 4C11) and anti-V3 MAbs (KD-247, 3E4, and 0.5γ) to cell surface-expressed Env proteins on HIV-$1_{JR\text{-}FL}$ chronically infected PM1 cells was analyzed by fluorescence-activated cell sorting. Comparisons of the binding profiles of the Abs to the cell surfaces were carried out using the mean fluorescence intensity (MFI). The binding of CD4i MAb 17b increased gradually as the amount of the CD4-mimicking small compound NBD-556 increased from 0 to 90 μM (Fig. 2A, the MFI increased from 68.36 to 320.73). As shown in Fig. 2C, the binding of both CD4i MAbs 17b and 4C11 increased remarkably after pretreatment with 100 μM NBD-556 (the MFIs increased from 43.3 to 201.57 and from 24.43 to 96.06, respectively). Moreover, the binding of all of the anti-V3 MAbs—KD-247, 3E4, and 0.5γ—was enhanced by pretreatment with NBD-556 (the MFIs increased from 34.59 to 51.9, from 22.97 to 39.07, and from 86.61 to 145.08, respectively). sCD4 pretreatment of the Env-expressing cell surface also caused remarkable enhancement of the binding for not only the CD4i MAbs but also the three anti-V3 MAbs, similar to pretreatment with NBD-556. These results indicate that the CD4-mimicking compound NBD-556 can induce the conformational changes in gp120 that are caused by binding of sCD4.

Highly synergistic interactions of KD-247 combined with NBD-556. Both neutralizing anti-V3 MAb KD-247 and NBD-556 block the viral entry process, especially at the stage of the interaction between CD4 and gp120 (CD4-binding site). Each of these agents binds to either the V3 loop or the CD4 cavity. Furthermore, our previous observations suggested that neu-

TABLE 2. Combination indices for KD-247, 4C11, or 0.5δ and for sCD4 or NBD-556 against HIV-1_{JR-FL} and HIV-1_{IIIB}

Combination	Virus	CI values at different ICs[a]		
		IC_{50}	IC_{75}	IC_{90}
KD-247+sCD4	HIV-1_{JR-FL}	0.313	0.266	0.277
KD-247+NBD-556	HIV-1_{JR-FL}	0.174	0.043	0.011
4C11+NBD-556	HIV-1_{IIIB}	0.473	0.445	0.860
0.5δ+NBD-556	HIV-1_{IIIB}	47.8	20.1	8.56

[a] The multiple-drug effect analysis of Chou et al. (6) was used to analyze the effects of the drugs in combination. IC, inhibitory concentration. CI < 0.9, synergy; CI = 0.9 to 1.1, additivity; CI > 1.1, antagonism. The data shown are representative of two or three separate experiments.

TABLE 3. Inhibitory activities of NBD-556 and sCD4 toward infection of HIV-1_{IIIB} escape variants from NBD-556 and sCD4

Virus	IC_{50}[a]	
	NBD-556 (μM)	sCD4 (μg/ml)
HIV-1_{IIIB}	12	0.52
HIV-$1_{NBD-R(20)14p}$	>30	5.7
HIV-$1_{NBD-R(50)17p}$	>30	>10
HIV-$1_{sCD4-R(20)5p}$	>30	>10

[a] PM1/CCR5 cells (2×10^3) were exposed to 100 $TCID_{50}$ of each passaged virus and then cultured in the presence of various concentrations of sCD4 or NBD-556. The IC_{50}s were determined by using the MTT assay on day 7 of culture. All assays were conducted in duplicate. The data shown are representative of two or three separate experiments.

tralizing MAb KD-247 selects escape variants with greater sensitivities to sCD4 (33). Based on this notion, we examined the synergy of this MAb with sCD4 or the CD4-mimicking compound NBD-556 against wild-type HIV-1_{JR-FL}. The multiple-drug effect analysis of Chou et al. (6) was used to analyze the effects of combining KD-247 with sCD4 or NBD-556. As shown in Table 2, all of the CI values for KD-247 with the two CD4-gp120 interaction inhibitors (sCD4 and NBD-556) were <0.5 against HIV-1_{JR-FL} at all of the inhibitory concentrations tested. In particular, the CI values for the combinations of KD-247 with NBD-556 were <0.1 for IC_{75} and IC_{90}. These results suggest that combinations of KD-247 with the CD4-gp120 binding inhibitors sCD4 and NBD-556 produce very highly synergistic effects. We further examined the synergy of CD4i MAb 4C11 or anti-CD4bs MAb 0.5δ with NBD-556 against wild-type HIV-1_{IIIB}. The combination of 4C11 and NBD-556 showed synergy against HIV-1_{IIIB} for IC_{50} and IC_{75}. As expected, the IC values for NBD-556 and anti-CD4 binding site MAb, 0.5δ, which may compete with the CD4 mimetic for the CD4-binding site, were >5 against HIV-1_{IIIB} at all of the inhibitory concentrations tested. However, at lower concentrations, additive effects were observed between NBD-556 and anti-CD4bs MAb 0.5δ (data not shown). These results indicate that NBD-556 may bind within or near the epitope of the anti-CD4bs MAb and then induce the conformational changes in Env.

Selection of NBD-556 and sCD4 escape variants. To select NBD-556- and sCD4-resistant HIV-1 variants *in vitro*, we exposed PM1/CCR5 cells to HIV-1_{IIIB} and serially passaged the viruses in the presence of increasing concentrations of NBD-556 or sCD4. As a control, HIV-1_{IIIB} was passaged under the same conditions without the antiviral agents to allow us to monitor the spontaneous changes that occurred in the virus during prolonged PM1/CCR5 cell passages (designated the passage control). The selected viruses were initially propagated in the presence of 1 μM NBD-556 or 0.5 μg of sCD4/ml and, during the course of the selection procedure, the concentrations of the NBD-556 and sCD4 were increased to 50 μM and 20 μg/ml, respectively. At passages 14 and 17 for NBD-556 and passage 5 for sCD4, the supernatants containing the viruses, which were designated HIV-$1_{NBD-R(20)14p}$, HIV-$1_{NBD-R(50)17p}$, and HIV-$1_{sCD4-R(20)5p}$, respectively, were harvested, and the sensitivities of the viruses to NBD-556 and sCD4 were determined by the MTT assay (Table 3). The IC_{50}s for NBD-556 against HIV-1_{IIIB}, HIV-$1_{NBD-R(20)14p}$, and HIV-$1_{NBD-R(50)17p}$ were 12, >30, and >30 μM, respectively. The IC_{50}s of sCD4 against HIV-1_{IIIB} and HIV-$1_{sCD4-R(20)5p}$ were 0.52 and >10 μg/ml, respectively. HIV-$1_{NBD-R(20)14p}$, HIV-$1_{NBD-R(50)17p}$, and HIV-$1_{sCD4-R(20)5p}$ were also examined for their cross-resistance with one another. Each resistant variant was found to be cross-resistant to NBD-556 and sCD4 (Table 3). These results indicate that the HIV-1_{IIIB} virus acquired resistant phenotypes against NBD-556 and sCD4 during the distinct *in vitro* selection processes.

Sequences of the envelope region of the NBD-556 and sCD4 mutants. To determine the genetic basis of the resistance in the variant HIV-1_{IIIB} strains, the C1 to C4 region of the *env* gene was amplified from genomic DNA extracted from the infected cells and cloned, and the PCR-amplified products were sequenced (Fig. 3). At passage 8 for 6 μM NBD-556, five mutations (A281D, E370A, S375N, A433T, and A436T) were observed. At passage 21 in the culture where HIV-1_{IIIB} was propagating in the presence of 50 μM NBD-556, four amino acid substitutions of Ser to Asn at position 375 (S375N, 11 of 11 clones) in C3, Ala to Lys at position 342 (A432K, 1 of 11 clones) in C4, Ala to Thr at position 433 (A433T, 4 of 11 clones) in C4, and Ala to Thr at position 436 (A436T, 1 of 11 clones) in C4 were observed (Fig. 3A). These results did not contradict a previous study in which gp120 mutants (S375W, I424A, W427A, and M475A) with changes in residues that contacted the Phe43 cavity did not detectably bind NBD-556 by isothermal titration calorimetry (23). On the other hand, in the selection with sCD4, seven mutations (E211G, P212L, V255E, N280K, S375N, G380R, and G431E) appeared during the passages. At passage 5 in the culture where HIV-1_{IIIB} was propagating in the presence of sCD4 (20 μg/ml), four substitutions of E211G (1 of 10 clones), V255E (5 of 10 clones), G380R (1 of 10 clones), and G431E (2 of 10 clones) were detected for sCD4 at 20 μg/ml (Fig. 3B).

To compare the two mutation profiles obtained during the *in vitro* selection with NBD-556 and sCD4, molecular modeling of NBD-556 docked into gp120 was performed by docking simulations using the FlexSIS module of SYBYL 7.1 (Fig. 4). The atomic coordinates of the crystal structure of gp120 with sCD4 were retrieved from the PDB (entry 1RZJ). As shown in Fig. 4, almost all of the mutations lay along the inside of the CD4 cavity in the selection of NBD-556, with similar three-dimensional positions to the mutations induced by sCD4. These findings demonstrate that NBD-556 binds to the CD4 cavity or in the vicinity of the CD4-binding site.

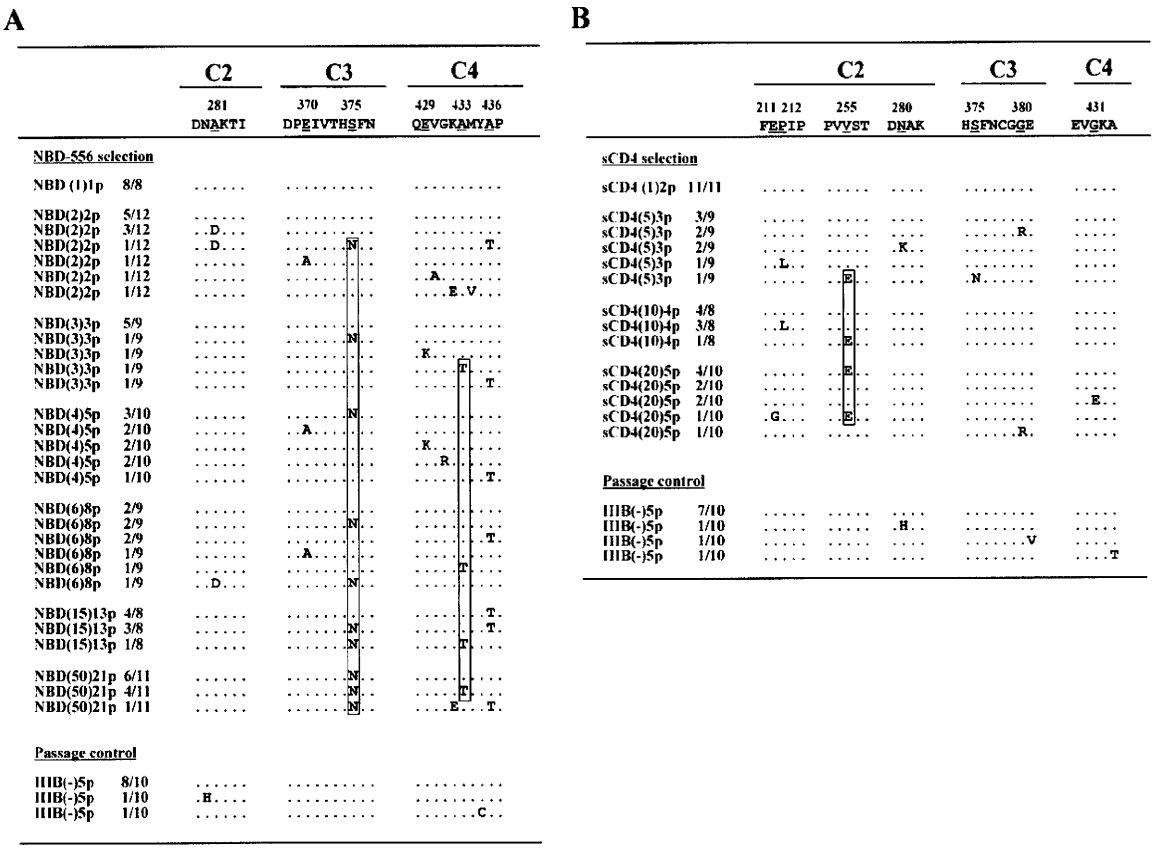

FIG. 3. Alignment of the gp120 amino acid sequences from the indicated passages in the NBD-556 and sCD4 escape processes. The amino acid sequences were deduced from the nucleotide sequences of the *env*-encoding regions of proviral DNA isolated from cells infected with the HIV-1_{IIIB} variants selected in the presence of NBD-556 (A) or sCD4 (B) and the passage control. The amino acid sequences of the envelope proteins of the baseline HIV-1_{IIIB} are shown at the top as a reference. The identity of the sequences at the individual amino acid positions is indicated by dots. The numbers of clones with the given amino acid substitutions among a total of 8 to 12 clones are listed. The number in parentheses denotes the concentrations of NBD-556 or sCD4. The major mutations of NBD-556 and sCD4-resistant variants at final passage are boxed.

Sensitivities of β-galactosidase reporter HIV strains pseudotyped with the sCD4- and NBD-556-resistant envelope mutations to NBD-556, sCD4, and MAbs. To confirm whether the mutations were responsible for the reduced sensitivities to NBD-556 and sCD4, a single-round replication assay was performed. The β-galactosidase reporter viruses were pseudotyped with wild-type Env (HIV-1_{WT}) or Env singly mutated with V255E in C2 (HIV-1_{V255E}), S375N in C3 (HIV-1_{S375N}), and A433T in C4 (HIV-1_{A433T}). The mutations that arose in the absence of NBD-556 (the passage control) are not related to resistance because the control passage did not show any significant increase in IC_{50} (data not shown). With respect to the mutations in the presence of NBD-556 three mutations, S375N, V255E, and A433T were consistently and increasingly observed during the process of selection. Additional mutations in "escape variants" other than S375N, V255E, and A433T were observed; however, these mutations were not consistently detected in passages and did not accumulate during selection. Thus, we considered the three mutations—S375N, V255E, and A433T—related to the development of resistance to both NBD-556 and sCD4, although some involvement of additional mutations in the development of a resistant phenotype is undeniable. As shown in Fig. 5A, all of the mutant clones were completely resistant to NBD-556 at concentrations of up to 20 μM. YYA-004 without the *p*-chlorophenyl group was unable to inhibit infection of all of the clones tested (Fig. 5B). The clone with V255E, which was induced by *in vitro* selection with sCD4, was highly resistant to sCD4 compared to the wild-type virus (114-fold-higher IC_{50}) (Fig. 5C). However, the other pseudotyped viruses, HIV-1_{S375N} and HIV-1_{A433T}, were slightly resistant compared to HIV-1_{WT} (4- and 2-fold-higher IC_{50}s, respectively). We also examined the sensitivities of the pseudotyped clones containing Env mutations to anti-gp120 glycan MAb 2G12, anti-CD4bs MAb b12, and anti-CD4 MAb RPA-T4 by a single-round replication assay (Fig. 5D to F). All of the mutant viruses showed almost the same neutralization sensitivities as the wild-type virus to the 2G12, b12, and RPA-T4 MAbs. These results indicate that the three mutations induced by *in vitro* selection with NBD-556 and sCD4 were responsible for the resistance to NBD-556, whereas the NBD-selected variants containing S375N in C3 and A433T in C4 of gp120 had moderately resistant phenotypes against sCD4, as shown by the sensitivities of the NBD-556-passaged viruses to sCD4 determined by the multiround assay (Table 3).

To examine whether the resistance mutations affected the sensitivity of a CD4i MAb against HIV-1, we determined the

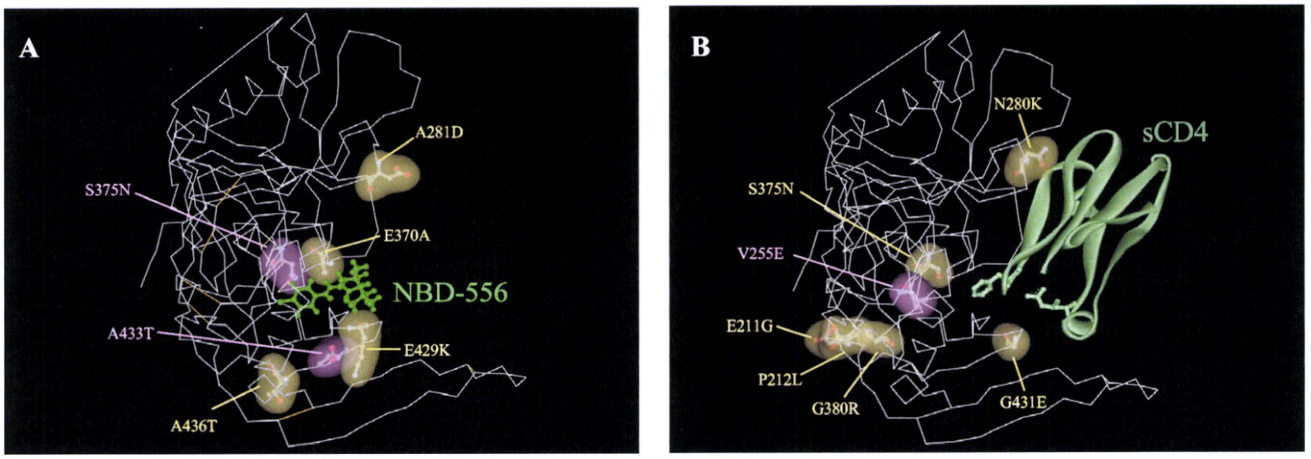

FIG. 4. Locations of substitutions in HIV-1_{IIIB} gp120 induced by *in vitro* selection with NBD-556 or sCD4. The side chains of the mutated residues that appeared during the *in vitro* selection with NBD-556 (A) or sCD4 (B) are shown in yellow and purple. The amino acid substitutions that confer resistance in HIV-1 are indicated in purple. The crystal structure of gp120 with sCD4 was retrieved from the PDB (entry 1RZJ). The structure of compound NBD-556 docked into gp120 was created by using the FlexSIS module of SYBYL 7.1.

sensitivities of HIV strains pseudotyped with the sCD4- and NBD-556-resistant envelope mutations to CD4i MAb 4C11 with or without the CD4-mimicking compound. As expected, NBD-556-pretreated HIV-1_{WT} was more sensitive to 4C11 than the untreated virus (IC_{50}s, 0.12 versus 0.72 μg/ml) (Fig. 6). On the other hand, all of the mutant viruses were completely resistant to 4C11 with or without NBD-556 pretreatment. These results suggest that the CD4 and NBD-556 resistance mutations in gp120 hide the epitope for a particular Ab against a CD4-induced epitope, similar to primary R5 viruses.

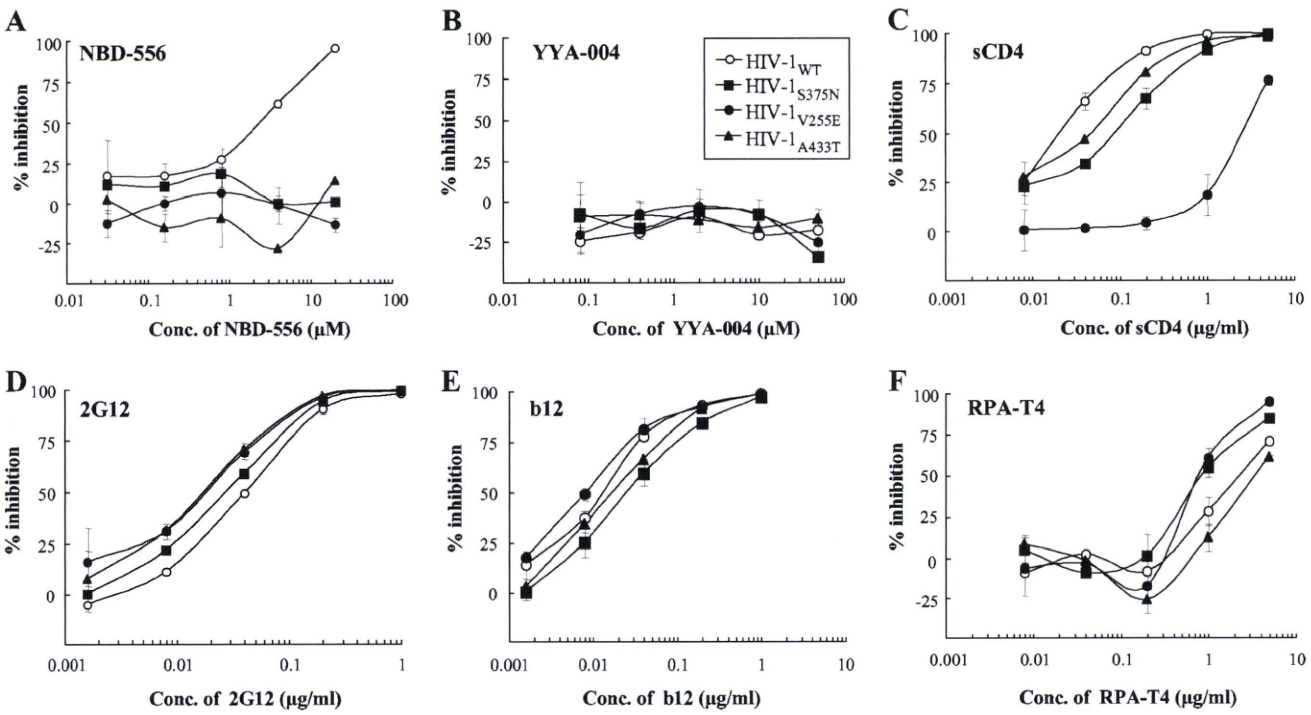

FIG. 5. Sensitivities of β-galactosidase reporter HIV strains pseudotyped with the sCD4 and NBD-556 resistance envelope mutations to NBD-556, YYA-004, sCD4, and MAbs. The sensitivities of β-galactosidase reporter HIV strains pseudotyped with the sCD4 and NBD-556 resistance envelope mutations to NBD-556 (A), YYA-004 (B), sCD4 (C), 2G12 (D), b12 (E), and RPA-T4 (F) are shown. NBD-556, YYA-004, sCD4, and MAbs at various concentrations and a pseudovirus suspension corresponding to 100 $TCID_{50}$ were preincubated for 15 min on ice and then added to the target cells (TZM-bl). The inhibitory effects were determined by measuring the β-galactosidase activities on day 2 of culture. All assays were conducted in triplicate, and the data shown represent the means ± the standard deviations (SD) derived from the results of two to three independent experiments.

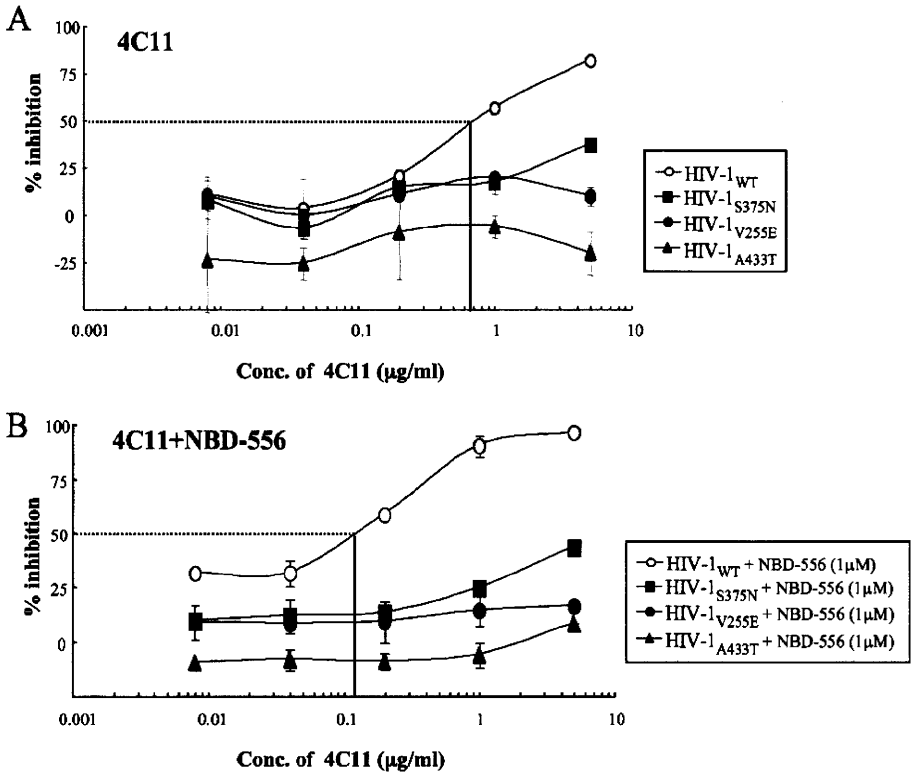

FIG. 6. Sensitivities of β-galactosidase reporter HIV strains pseudotyped with the sCD4 and NBD-556 resistance envelope mutations to CD4i MAb 4C11 with or without NBD-556. The sensitivities of β-galactosidase reporter HIV strains pseudotyped with the sCD4 and NBD-556 resistance envelope mutations to CD4i MAb 4C11 in the absence (A) or presence (B) of NBD-556 are shown. 4C11 at various concentrations and a pseudovirus suspension corresponding to 100 $TCID_{50}$ were preincubated with or without NBD-556 (1 μM) for 15 min on ice and then added to the target cells (TZM-bl). The inhibitory effects were determined by measuring the β-galactosidase activities on day 2 of culture. All assays were conducted in triplicate, and the data shown represent the means ± the SD derived from the results of two to three independent experiments.

NBD-556-mediated enhancement of the neutralization activities of plasma Abs against an autologous isolate. Neutralization escape has been documented in HIV-1 subtype B viruses, with contemporaneous viruses showing less sensitivity to autologous neutralization than earlier viruses (2). For one patient (patient 3 [Pt.3]) infected with a subtype B virus, the autologous neutralizing activities in plasma IgG obtained close to the time of the virus isolation were measured in the presence or absence of NBD-556 (0, 1, 2, 4, and 8 μM) by the MTT assay. As shown in Fig. 7A, the plasma IgG neutralizing activity was much less potent against the variant ($HIV\text{-}1_{Pt.3}$) from the same time point (IC_{50} of >200 μg/ml for IgG). However, $HIV\text{-}1_{Pt.3}$ pretreated with at least 1 μM NBD-556 became sensitive to the contemporaneous plasma IgG compared to the untreated virus. To examine which kinds of NAbs are enhanced by NBD-556, we determined the susceptibilities of $HIV\text{-}1_{Pt.3}$ to anti-V3 MAb KD-247 and CD4i MAb 4E9C with or without NBD-556. The virus was completely resistant to both MAbs (IC_{50}s of >100 μg/ml) in the absence of NBD-556, while NBD-556-pretreated $HIV\text{-}1_{Pt.3}$ became sensitive to KD-247 and 4E9C (IC_{50}s of 10.0 and 20.8 μg/ml, respectively) (Fig. 7B). These results indicate that CD4-mimicking small compounds such as NBDs have potent NAb-enhancing activities toward plasma Abs that cannot access the neutralizing epitopes hidden within the trimeric Env, such as CD4i and anti-V3 Abs.

DISCUSSION

In this study, we observed that NBD-556 could bind to a CD4-binding site, followed by the induction of conformational changes in gp120 similar to those observed upon sCD4 binding. Although we used a limited number of viruses and plasma IgG preparations obtained from an HIV-1-positive patient for testing the synergistic effects between NBD-556 and neutralizing antibody, we also found highly synergistic interactions between NBD-556 and not only CD4i MAbs but also anti-V3 MAbs. Moreover, our data indicated that small compounds such as NBDs can enhance the potency of NAbs in HIV-1-infected patients against the contemporaneous viruses, which are resistant to neutralization by Abs in the plasma.

We illustrated the sites of the mutations induced by NBD-556 on the structure of unliganded gp120 of SIV obtained from the PDB (entry 2BF1) to compare the sites before and after binding of the CD4-mimicking compound. As shown in Fig. 8, the mutations lay in front of the outer domain in gp120, which was near to or within the CD4-binding site. These findings indicate that NBD-556 attaches to the CD4-binding site or the

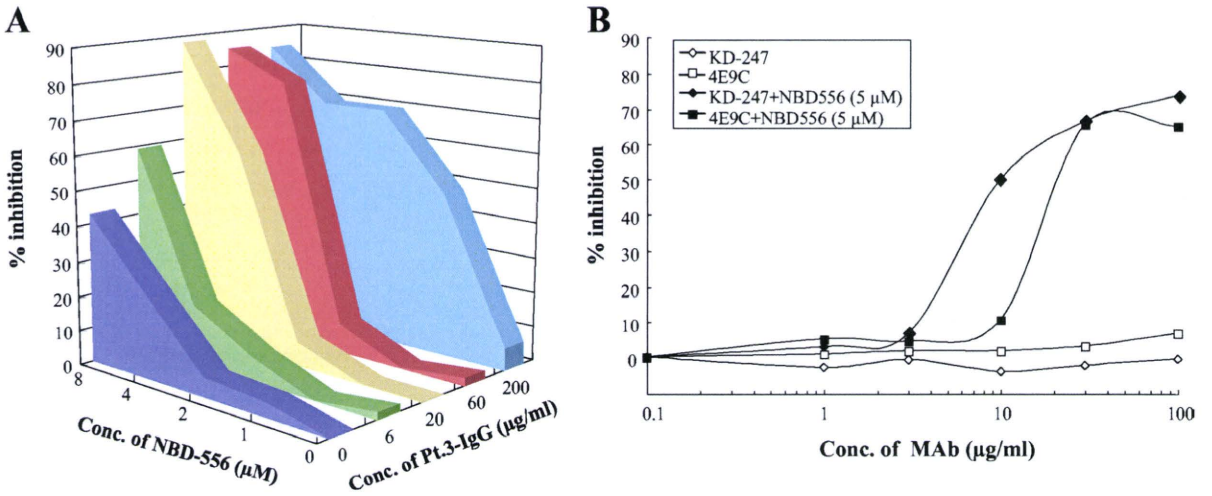

FIG. 7. NBD-556-mediated enhancement of the neutralization activity of plasma IgG against the autologous isolate. (A) The sensitivities of the HIV-$1_{Pt.3}$ primary isolate to the autologous plasma IgG (Pt.3-IgG) in the absence or presence of NBD-556 (1, 2, 4, and 8 μM) were determined by the MTT assay. (B) The sensitivities of the HIV-$1_{Pt.3}$ primary isolate to KD-247 (anti-V3 MAb; diamonds) and 4E9C (anti-CD4i MAb; squares) in the absence (open symbols) or presence (filled symbols) of 5 μM NBD-556 were determined by the same assay. The data shown are representative of two or three separate experiments.

surrounding residues in the unliganded form of gp120 and that, after the conformational changes of the envelope glycoproteins, probably the CD4-liganded form induced by the attack by NBD-556, the compound could penetrate and be held for a while in the CD4 cavity. In a recent study, Haim et al. (14) showed that sCD4-mimicking compounds have the ability to inactivate HIV-1 by prematurely triggering active but transient intermediate states of the envelope glycoproteins. In the transient intermediate states, several neutralizing epitopes in gp120 may be accessible to the neutralizing Abs. These data and our present results suggest that some NBD analogs, which bind to the cavity tightly and for a longer time, as well as cell surface CD4 inducing a more stable envelope glycoprotein intermediate state, show highly potent NAb-enhancing activities.

Madani et al. (23) reported that replacement of gp120 Ser375 with a glycine residue dramatically reduced the HIV-1 sensitivity to enhancement by any of the NBD-556 analogs, suggesting that a certain element of the Ser375 side chain contributes to the NBD-556 efficacy. They also reported that viruses bearing envelope glycoproteins with Ser375 mutated to alanine exhibited greater enhancement by NBD-556 and some NBD-556 analogs than the viruses with wild-type envelope glycoproteins, suggesting that the hydroxyl group of Ser375 is detrimental to the binding and/or activity of some NBD-556 analogs that contain large para-phenyl substituents. Mutations

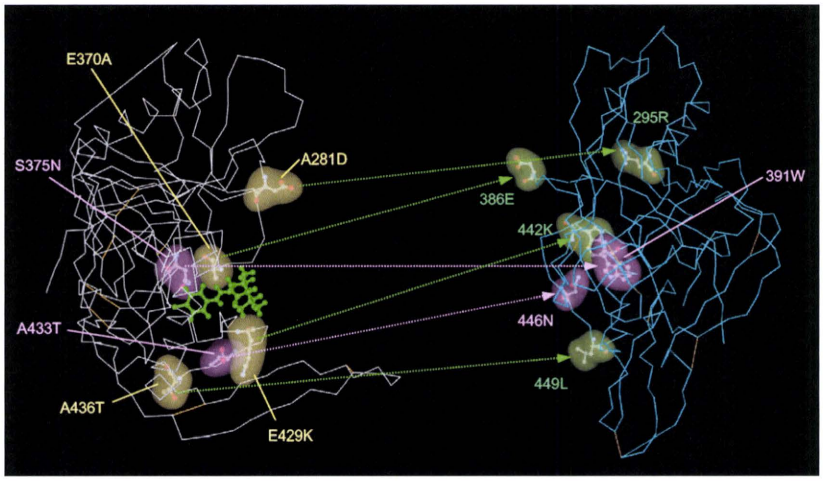

FIG. 8. Comparisons of the locations of the mutations induced by NBD-556 between the structures of unliganded and liganded gp120. The side chains of the mutated residues that appeared during *in vitro* selection with NBD-556 are shown in yellow, green and purple in the liganded (left) or unliganded (right) structures. The amino acid substitutions that confer resistance in HIV-1 are indicated in purple (S375N and A433T). The crystal structures of liganded and unliganded gp120 were retrieved from the PDB (entries 1RZJ and 2BF1, respectively). The corresponding sites of the NBD-resistant mutations are also shown on the unliganded gp120.

of other gp120 residues lining the Phe43 cavity or vestibule (Val255, Thr257, Glu429, and Val430) significantly decreased the enhancement of virus infection by the NBD-556 analogs. Our *in vitro* selection study showed that the key mutations for NBD-556 resistance were S375N and A433T and that minor mutations related to NBD-556 resistance were A281D, E370A, E429K, and A436T (Fig. 4). Thus, alterations to several gp120 residues, namely, S375N, A433T, and V255E, that line the Phe43 pocket or reside around and inside the cavity can negatively affect the entry inhibitory effect of NBD-556 on HIV-1 infection (Fig. 5).

Decker et al. (9) reported that the chemokine coreceptor binding sites of HIV-1 from subtypes A, B, C, D, F, G, and H and circulating recombinant form (CRF) 01, CRF02, and CRF11 elicit high titers of CD4i Abs during natural human infection and that these Abs bind and neutralize viruses as divergent as HIV-2 in the presence of sCD4. Recently, Davis et al. (7) showed that transplantation of HIV-1 V3 epitopes into an HIV-2 envelope scaffold provides a sensitive and specific means to detect and quantify HIV-1 V3 epitope-specific NAbs in human sera. They used this HIV-2/HIV-1 V3 scaffolding strategy to study the kinetics of the development and breadth of V3-specific NAbs in longitudinal sera from individuals acutely infected with subtype C or subtype B HIV-1. Their results indicated that high-titer broadly reactive V3-specific Abs are among the first to be elicited during acute and early HIV-1 infection, although these Abs lack neutralizing potency against primary HIV-1 viruses, which effectively shield V3 from Ab binding to the functional Env trimer (8). These observations strongly support the idea that the major problem facing the development of CD4i-based or V3-based immunogens is not sequence variation within the epitopes, but rather that access of most CD4i and anti-V3 Abs to their epitopes in functional Env complexes is blocked. As shown in Fig. 7A, plasma IgG from a seropositive patient exhibited strongly enhanced neutralizing activity against the contemporaneous virus after treatment with NBD-556. Therefore, we consider that small compounds such as NBDs can enhance the neutralizing activities of CD4i and certain anti-V3 Abs *in vivo* at the acute stage of HIV-1 infection or in combination with anti-V3 NAbs as a passive immunization.

In general, small molecules have certain advantages from a therapeutic standpoint because of their low propensity for immunogenicity, high metabolic stability, easy large-scale production, and relatively low cost. Small molecule Ab-enhancing therapeutics such as NBD compounds would have additional benefits over available treatment approaches to HIV. Since CD4i and anti-cryptic V3 Abs are already present in a large number of HIV-1-infected patients, no prevaccination would be necessary for the induction of NAbs. Moreover, the use of bifunctional small molecules, such as an entry inhibitor and a NAb enhancer, should be effective for passive immunization of the anti-HIV NAbs enhanced by the accessibility of epitopes after binding of sCD4, such as 17b (27) and KD-247 (11, 12). Elucidation of the molecular details governing the interactions between gp120 and NBD compounds will assist in optimization efforts, as well as in the evaluation of this strategy in more complex biological models for HIV infection. Consequently, we will continue to synthesize such NBD analogs to search for drugs with more potent power to change the tertiary structure of the envelope glycoproteins and lower toxicity toward the host cells.

ACKNOWLEDGMENTS

We thank The Chemo-Sero-Therapeutic Research Institute for kindly providing MAb KD-247. We are grateful to Yosuke Maeda for providing the PM1/CCR5 cells. We also thank Akiko Honda-Shibata, Yoko Kawanami, and Syoko Yamashita for excellent technical assistance.

This study was supported in part by the Ministry of Health, Labor, and Welfare of Japan (H20-AIDS-002 and H21-AIDS-010); a Grant-in-Aid for Scientific Research (C-20591206) from the Ministry of Education, Science, and Culture of Japan; and the Cooperative Research Project on Clinical and Epidemiological Studies of Emerging and Re-emerging Infectious Diseases.

REFERENCES

1. **Blish, C. A., R. Nedellec, K. Mandaliya, D. E. Mosier, and J. Overbaugh.** 2007. HIV-1 subtype A envelope variants from early in infection have variable sensitivity to neutralization and to inhibitors of viral entry. AIDS **21:** 693–702.
2. **Bunnik, E. M., L. Pisas, A. C. van Nuenen, and H. Schuitemaker.** 2008. Autologous neutralizing humoral immunity and evolution of the viral envelope in the course of subtype B human immunodeficiency virus type 1 infection. J. Virol. **82:**7932–7941.
3. **Burton, D. R.** 2002. Antibodies, viruses, and vaccines. Nat. Rev. Immunol. **2:**706–713.
4. **Burton, D. R., R. C. Desrosiers, R. W. Doms, W. C. Koff, P. D. Kwong, J. P. Moore, G. J. Nabel, J. Sodroski, I. A. Wilson, and R. T. Wyatt.** 2004. HIV vaccine design and the neutralizing antibody problem. Nat. Immunol. **5:**233–236.
5. **Burton, D. R., R. L. Stanfield, and I. A. Wilson.** 2005. Antibody versus HIV in a clash of evolutionary titans. Proc. Natl. Acad. Sci. U. S. A. **102:**14943–14948.
6. **Chou, T. C., and P. Talaly.** 1977. A simple generalized equation for the analysis of multiple inhibitions of Michaelis-Menten kinetic systems. J. Biol. Chem. **252:**6438–6442.
7. **Davis, K. L., F. Bibollet-Ruche, H. Li, J. M. Decker, O. Kutsch, L. Morris, A. Salomon, A. Pinter, J. A. Hoxie, B. H. Hahn, P. D. Kwong, and G. M. Shaw.** 2009. Human immunodeficiency virus type 2 (HIV-2)/HIV-1 envelope chimeras detect high titers of broadly reactive HIV-1 V3-specific antibodies in human plasma. J. Virol. **83:**1240–1259.
8. **Davis, K. L., E. S. Gray, P. L. Moore, J. M. Decker, A. Salomon, D. C. Montefiori, B. S. Graham, M. C. Keefer, A. Pinter, L. Morris, B. H. Hahn, and G. M. Shaw.** 2009. High titer HIV-1 V3-specific antibodies with broad reactivity but low neutralizing potency in acute infection and following vaccination. Virology **387:**414–426.
9. **Decker, J. M., F. Bibollet-Ruche, X. Wei, S. Wang, D. N. Levy, W. Wang, E. Delaporte, M. Peeters, C. A. Derdeyn, S. Allen, E. Hunter, M. S. Saag, J. A. Hoxie, B. H. Hahn, P. D. Kwong, J. E. Robinson, and G. M. Shaw.** 2005. Antigenic conservation and immunogenicity of the HIV coreceptor binding site. J. Exp. Med. **201:**1407–1419.
10. **Derdeyn, C. A., J. M. Decker, F. Bibollet-Ruche, J. L. Mokili, M. Muldoon, S. A. Denham, M. L. Heil, F. Kasolo, R. Musonda, B. H. Hahn, G. M. Shaw, B. T. Korber, S. Allen, and E. Hunter.** 2004. Envelope-constrained neutralization-sensitive HIV-1 after heterosexual transmission. Science **303:**2019–2022.
11. **Eda, Y., T. Murakami, Y. Ami, T. Nakasone, M. Takizawa, K. Someya, M. Kaizu, Y. Izumi, N. Yoshino, S. Matsushita, H. Higuchi, H. Matsui, K. Shinohara, H. Takeuchi, Y. Koyanagi, N. Yamamoto, and M. Honda.** 2006. Anti-V3 humanized antibody KD-247 effectively suppresses ex vivo generation of human immunodeficiency virus type 1 and affords sterile protection of monkeys against a heterologous simian/human immunodeficiency virus infection. J. Virol. **80:**5563–5570.
12. **Eda, Y., M. Takizawa, T. Murakami, H. Maeda, K. Kimachi, H. Yonemura, S. Koyanagi, K. Shiosaki, H. Higuchi, K. Makizumi, T. Nakashima, K. Osatomi, S. Tokiyoshi, S. Matsushita, N. Yamamoto, and M. Honda.** 2006. Sequential immunization with V3 peptides from primary human immunodeficiency virus type 1 produces cross-neutralizing antibodies against primary isolates with a matching narrow-neutralization sequence motif. J. Virol. **80:**5552–5562.
13. **Guex, N., A. Diemand, and M. C. Peitsch.** 1999. Protein modeling for all. Trends Biochem. Sci. **24:**364–367.
14. **Haim, H., Z. Si, N. Madani, L. Wang, J. R. Courter, A. Princiotto, A. Kassa, M. DeGrace, K. McGee-Estrada, M. Mefford, D. Gabuzda, A. B. Smith III, and J. Sodroski.** 2009. Soluble CD4 and CD4-mimetic compounds inhibit HIV-1 infection by induction of a short-lived activated state. PLoS Pathog. **5:**e1000360.